



저작자표시-비영리-변경금지 2.0 대한민국

이용자는 아래의 조건을 따르는 경우에 한하여 자유롭게

- 이 저작물을 복제, 배포, 전송, 전시, 공연 및 방송할 수 있습니다.

다음과 같은 조건을 따라야 합니다:



저작자표시. 귀하는 원저작자를 표시하여야 합니다.



비영리. 귀하는 이 저작물을 영리 목적으로 이용할 수 없습니다.



변경금지. 귀하는 이 저작물을 개작, 변형 또는 가공할 수 없습니다.

- 귀하는, 이 저작물의 재이용이나 배포의 경우, 이 저작물에 적용된 이용허락조건을 명확하게 나타내어야 합니다.
- 저작권자로부터 별도의 허가를 받으면 이러한 조건들은 적용되지 않습니다.

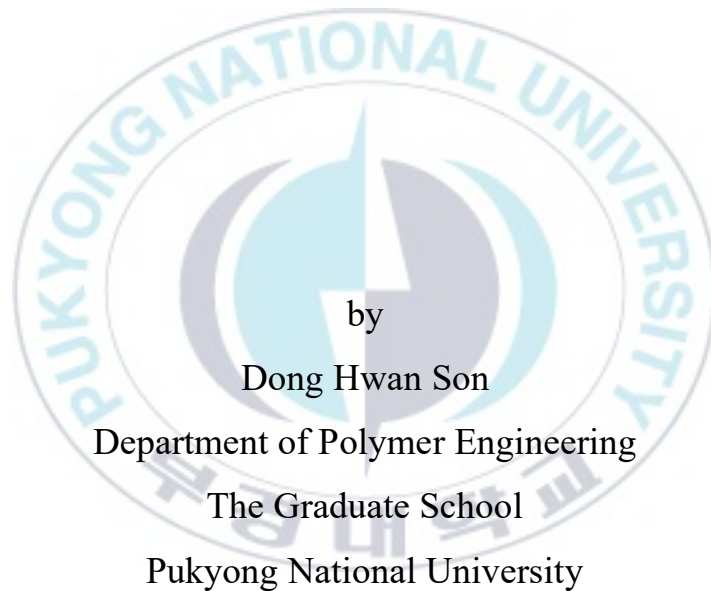
저작권법에 따른 이용자의 권리는 위의 내용에 의하여 영향을 받지 않습니다.

이것은 [이용허락규약\(Legal Code\)](#)을 이해하기 쉽게 요약한 것입니다.

[Disclaimer](#)

Thesis for the Degree of Master of Engineering

Synthesis of indandione-based Conjugated polymers for Polymer Solar Cells.

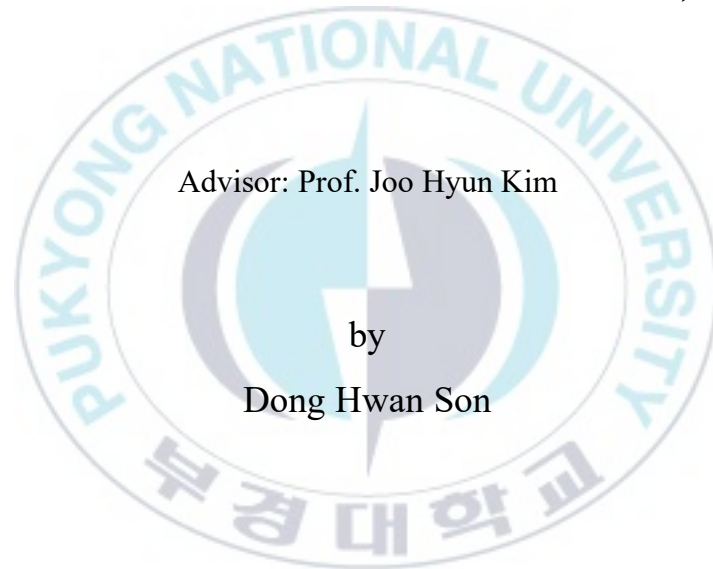


February, 2022

Synthesis of indandione-based Conjugated
polymers for Polymer Solar Cells.

(고분자 태양 전지를 위한 인단디온

기반의 공액고분자 합성)



A thesis submitted in partial fulfillment of the requirements
for the degree of Master of Engineering
in Department of Polymer Engineering, The Graduate School,
Pukyong National University

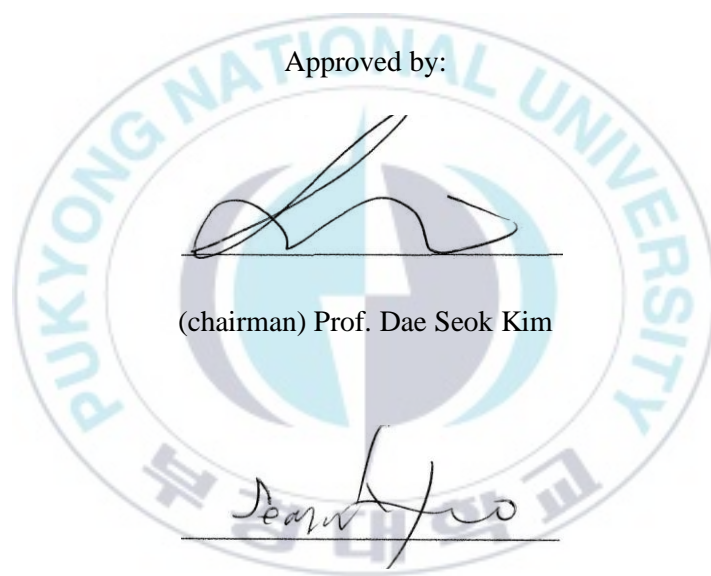
February, 2022

Synthesis of indandione-based Conjugated polymers for Polymer Solar Cells.

A thesis

A dissertation
By
Dong Hwan Son

Approved by:



(Member) Prof. Seong Il Yoo

(Member) Prof. Joo Hyun Kim

February 25, 2022

Contents

Chapter I Introduction	1
I.i Motivation	1
I.ii Polymer Solar Cells (OSCs)	2
I.iii Device Structures of PSCs	3
I.iii.1 Bilayer heterojunction PSCs	5
I.iii.2 Bulk Heterojunction (BHJ) OSCs	7
I.iv Principle of Solar PSCs	9
I.v General Parameters of Solar Cells	11
I.v.1.1 Short-circuit Current (J_{sc})	11
I.v.1.2 Open Circuit Voltage (V_{oc})	12
I.v.1.3 Fill Factor (FF)	13
I.v.1.4 Power Conversion Efficiency (PCE)	15
Chapter II Synthesis of 4,7-dibromo-1H-indene-1,3(2H)-dione based Conjugated polymers for Polymer Solar Cells	16
II.i Introduction	16
II.ii Experimental	18
II.ii.1 Materials	18
II.ii.2 Synthesis of IND-HT	19
II.ii.3 Synthesis of D-A type polymers by Stille coupling reaction ⁴²²²	22

II.ii.4	Measurement.....	25
II.ii.5	Fabrication of OSCs.....	26
II.iii	Results and discussion.....	28
II.iv	Morphology of the polymers and their blends.....	39
II.v	Conclusion	45
Chapter III	Effect of Dihexyl-thiophene with 4,7-dibromo-1H-indene-1,3(2H)-dione based Conjugated polymers as donor for Polymer Solar Cells.	46
III.i	Introduction.....	46
III.ii	Experimental.....	48
III.ii.1	Materials.....	48
III.ii.2	Synthesis of IND-DHT.....	49
III.ii.3	polymerization of D-A type polymers by Stille coupling reaction ⁴²	54
III.ii.4	Measurement.....	57
III.iii	Results and discussion.....	59
III.iii.1	Optical and Electrochemical Properties.	59
III.iii.2	Photovoltaic properties.....	62
III.iii.3	Computational calculation	65
III.iv	Conclusion.....	67
Ref.....	68
Acknowledgment.....	75

Figure I -I. Device Structure of Conventional and inverted PSC.....	4
Figure I-II. Structure of Bilayer heterojunction PSCs.....	6
Figure I-III. The generation process of photo-induced charges along with interpenetrating separated D-A network.....	8
Figure I-IV. Operating principles of organic photovoltaic device.....	10
Figure I-V. The typical current-voltage (I-V) curve of solar cells.....	14
Figure II-I. Thermal gravimetric analysis (TGA) curves of (a) IND-HT-BDT and (b) IND-HT-BDTF.....	29
Figure II-II. UV-visible spectra of polymer donors (a) thin films on glass substrates and (b) solution in chloroform and Cyclic voltammograms of (c) IND-HT-BDT, (d) IND-HT-BDTF and corresponding (e) energy diagram.....	31
Figure II-III. Current density vs. voltage curves of PSCs under 1.0 sun and dark condition on the PC71BM acceptor under optimum conditions and (b) Current density vs. voltage curves of PSCs under 1.0 sun and dark condition on the Y6BO under optimum conditions. (c) the corresponding incident photon-to-current efficiency (IPCE) curves of the OSCs based on polymer donors with PC71BM. (d) the corresponding incident photon-to-current efficiency (IPCE) curves of the OSCs based on polymer donors with Y6BO.....	35
Figure II-IV GIWAXS images of (a) neat IND-HT-BDT, IND-HT-BDTF, (b) polymer with PC71BM optimized blend film, and (c) polymer with Y6BO optimized blend film.....	42
Figure III-I UV-visible spectra of polymer donors (a) thin films on glass substrates and (b) solution in chloroform and Cyclic voltammograms	

of (c) IND-DHT-BDT, (d) IND-DHT-BDTF and corresponding (e) energy diagram..... 63

Figure III-II. The electronic distributions of polymer donors obtained from density functional theory (DFT) calculations..... 66



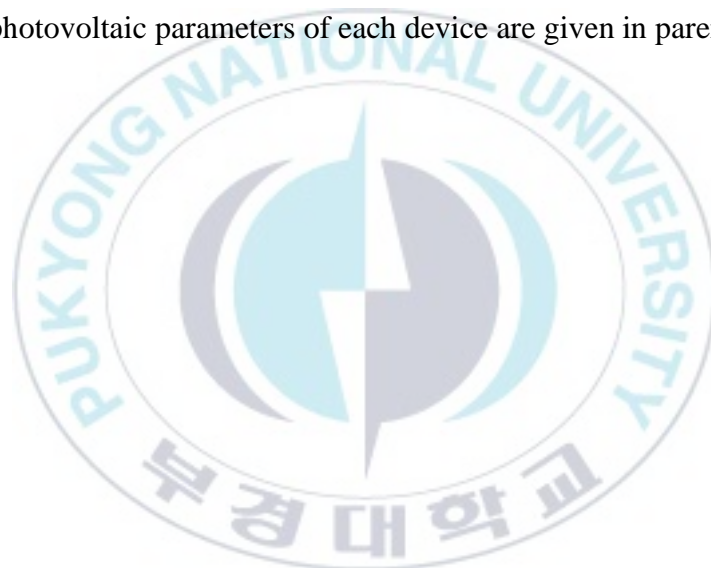
List of Table

Table I Summary of optical and electrochemical properties of the polymer.

Table II The best photovoltaic parameters of the PSCs. The averages for the photovoltaic parameters of each device are given in parentheses

Table III Summary of optical and electrochemical properties of the polymer.

Table IV The best photovoltaic parameters of the PSCs. The averages for the photovoltaic parameters of each device are given in parentheses



고분자 태양 전지를 위한 인단디온 기반의 공액고분자 합성

손 동 환

부경대학교 대학원 고분자공학과

요 약

대표적인 에너지원인 화석연료의 사용에 따른 화석 연료의 고갈과 환경 문제에 따라 대체 에너지의 개발이 중요시되고 있다. 그 중 태양광의 발전은 환경적인 문제나 별다른 기계적 장치 없이 직접적으로 전기를 생산이 가능하기에 오늘날 중요한 에너지원으로 꼽히고 있다. 이 중 유기태양전지는 투명하고 유연하며 가볍다는 특성을 가지기 때문에, 다양한 공간과 다양한 장소에 적용이 가능하며 휴대성도 좋다는 장점을 가진다. 또한 유기태양전지는 용액 공정으로 제작이 가능하기에 제작단가도 저렴하며 친환경적이다. 하지만 아직까지 낮은 효율성과 안정성 등으로 상용화에 어려움을 가진다. 이에 본 연구에서는 고분자 태양전지의 효율을 향상시키기 위해서 유기태양전지의 구조인 유리/인듐-주석 산화물(ITO)/산화아연(ZnO)/유기 광활성층/은(Ag) 중에서 유기 광활성층에 연구를 집중하였다. 유기 광활성층에 사용되는 물질 중 대표적으로 전자 수용체로 사용되는 fullerene 계 유도체인 PC₇₁BM 의 경우 에너지 준위를 조절할 수 없고 가시광선 영역의 흡수가 적으며 높은 순도로 정제하기 어려운 단점이 있다. 이를 개선한 물질인 non-fullerene 계 유도체인 Y6BO 의 경우, 가시광선 영역에서 큰 흡수 파장 범위를 가지며 말단기의 조절을 통해 에너지 준위를 조절하기가 쉽다는 장점을 가지기에 이를 전자 수용체로 선택을 하였으며, Y6BO 의 말단기에서 영감을 받아 indandione 을 기반으로 물질을 합성하였으며 이는 전자 수용체와 전자 공여체의 상용성을 증가시켰으며, 고분자의 용해도를 증가시키기 위해서 말단기에 hexyl 기를 도입하였으며, 전자의 이동성을 증가시키기 위해서 구조적 안정성 및 평면성의 특징을 가지는 BDT 및 BDTF 를 도입한 고분자를 만들고, 광전변환 특성을 평가하였다. 그 결과, 2 개의 전자 공여체 소재 중에서 IND-HT-BDTF 를 기반으로 하는 유기태양전지 소자가 최대 6.43%의 효율을 나타냈다.

Chapter I Introduction

I.i Motivation

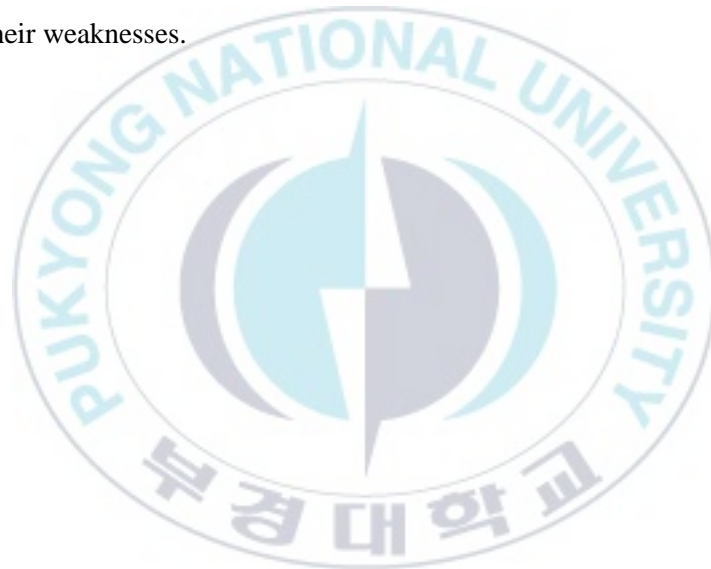
Fossil fuel has long been an important source of energy. As a consequence of using, several environmental problems have emerged, such as pollution, global warming¹, and an increase in water temperatures. For solving these problems, many clean energy systems have been developed.

Many researchers have attempted to fabricate solar cells using solar energy as a candidate for clean energy systems². Solar cells have many advantages, including renewable energy without chemical pollution, noise pollution, and greenhouse gases.

Furthermore, solar cells have a cost-saving effect due to their direct conversion of sunlight into electricity, long-term maintenance without any repairs, and no escalating fuel costs.

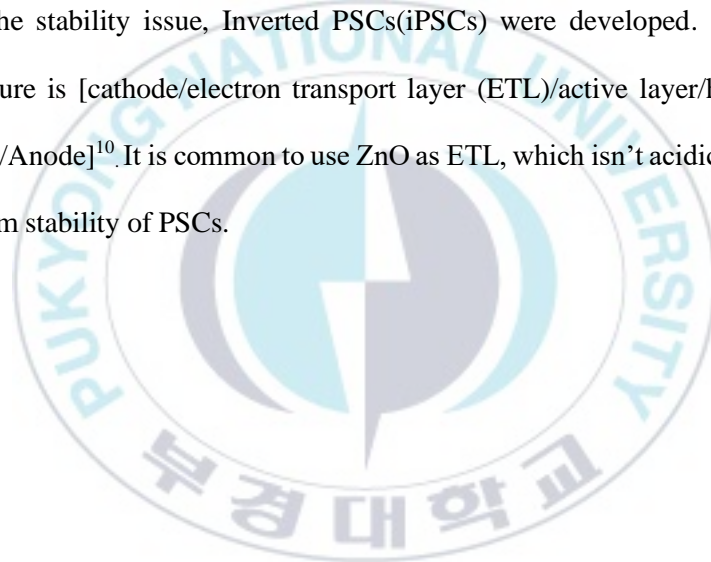
I.ii Polymer Solar Cells (OSCs)

Many types of solar cells were designed and developed such as silicon solar cells³, inorganic solar cells⁴, dye-sensitized solar cells⁵, organic solar cells⁶, and quantum dots solar cells⁷. But each has pros and cons, and researchers continue to find a way to overcome their weaknesses.



I.iii Device Structures of PSCs

The device structures of PSCs can be categorized as conventional or inverted types (shown in **Figure I - 1**). Conventional type PSCs structure is [anode/hole transport layer (HTL)/active layer/electron transport layer (ETL)/cathode]⁸. It is common to use PEDOT:PSS as HTL, which is acidic, affecting the long-term stability of PSCs⁹. To overcome the stability issue, Inverted PSCs (iPSCs) were developed. Inverted type PSCs structure is [cathode/electron transport layer (ETL)/active layer/hole transport layer (HTL)/Anode]¹⁰. It is common to use ZnO as ETL, which isn't acidic, can develop the long-term stability of PSCs.



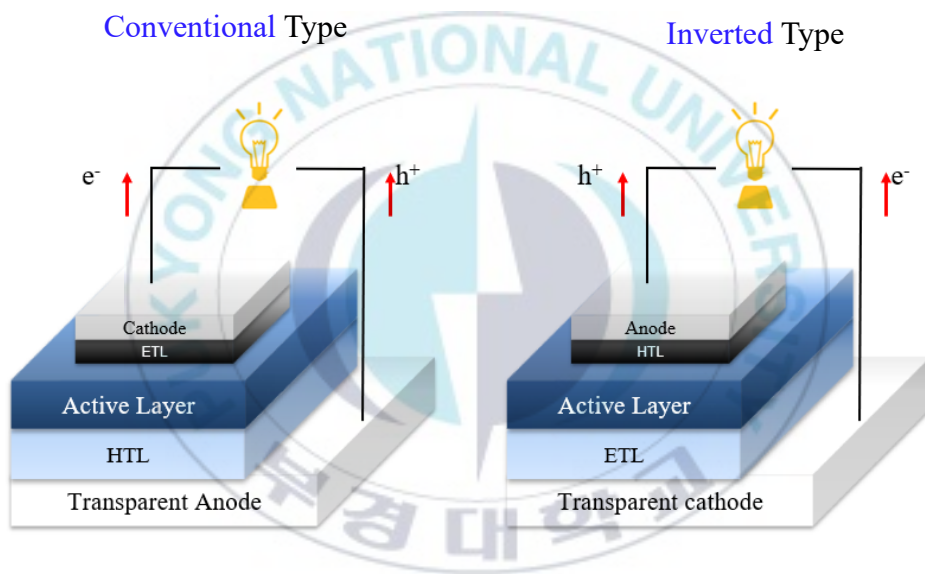


Figure I -II. Device Structure of Conventional and inverted PSC

I.iii.1 Bilayer heterojunction PSCs

The Bilayer type PSCs structure is a basic structure of PSCs (shown in **Figure I – 2**). Except for the electrode, the structure of the active layer is simply a stack of donors and acceptors. However, since the lifetime of exciton is less than a few nanometers, some electrons cannot move layer to layer and are recombined into excitons¹¹.



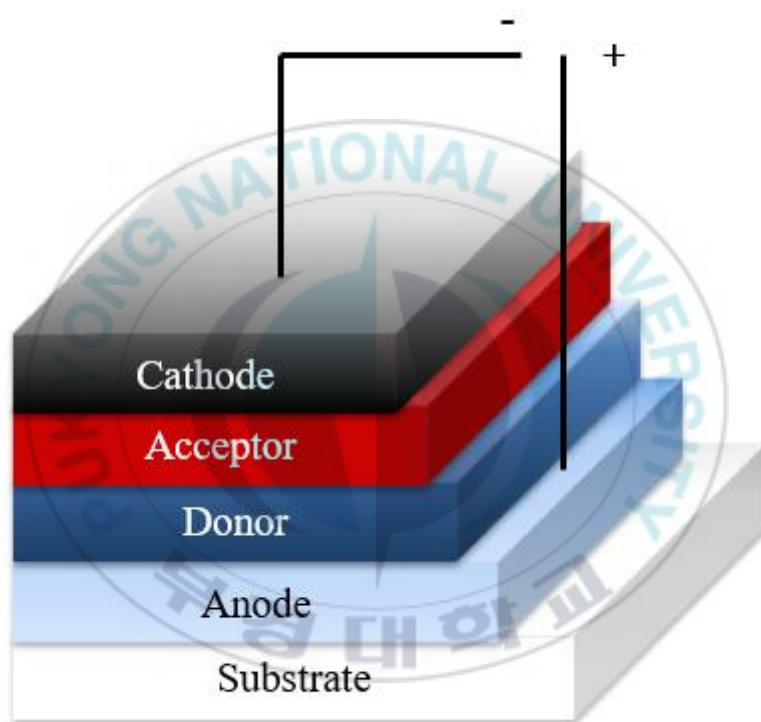
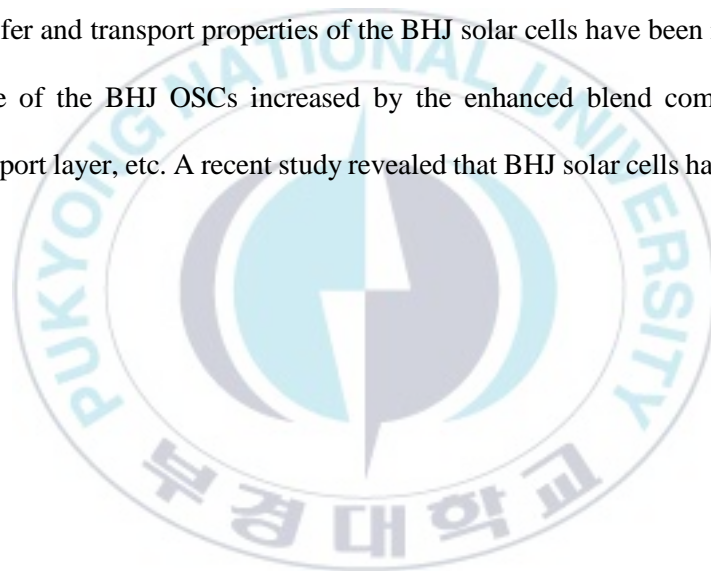


Figure I-III. Structure of Bilayer heterojunction PSCs

I.iii.2 Bulk Heterojunction (BHJ) OSCs

In 1995, donor-acceptor blend layers for BHJ OSCs were suggested to resolve bilayer heterojunction PSCs issues¹². BHJ is possible only in organic solar cells that can be processed in a solution (shown in **Figure I – 3**). BHJ solar cells were developed 27 years ago, even after that time, the basic structure of cells was kept intact, and the charge transfer and transport properties of the BHJ solar cells have been improved and performance of the BHJ OSCs increased by the enhanced blend composition, and charge transport layer, etc. A recent study revealed that BHJ solar cells had over 20%¹³.



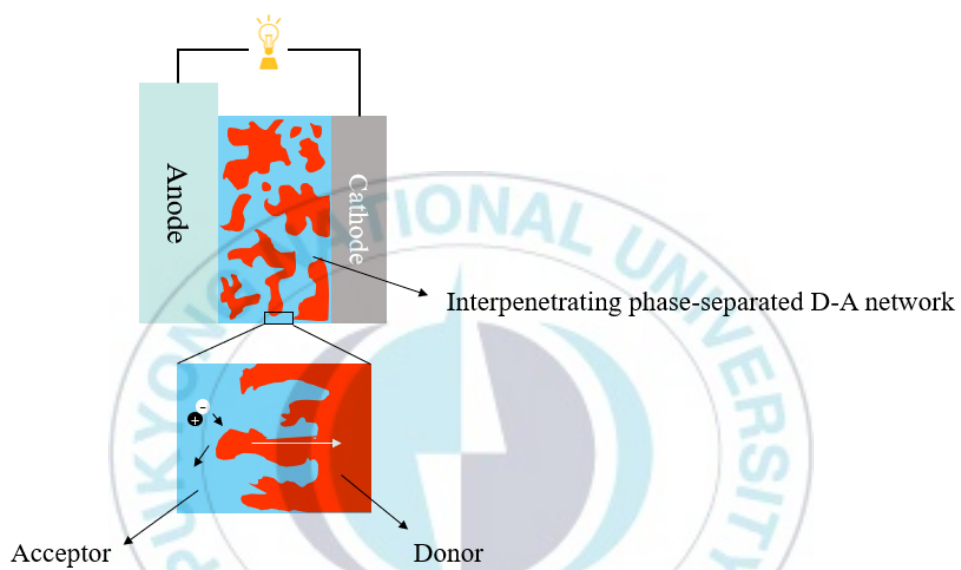


Figure I-IVVVI. The generation process of photo-induced charges along with interpenetrating separated D-A network

I.iv Principle of Solar PSCs

The four main steps of PSCs operation are exciton generation, exciton diffusion, charge separation, and charge collection (shown in **Figure I – 4**). (1) Exciton which is electron-hole pair is generated from light absorption in electron donor. (2) Exciton diffusion between electron donor and electron acceptor (D-A) interface. If the exciton's maximum diffusion length (~ 20 nm) is exceeded, the exciton will be relaxed. (3) Exciton at the interface between electron donor and electron acceptor dissociate electron and hole. (4) In case of electron pass through the HOMO of donor and ETL, hole passes through the LUMO of acceptor and HTL (5) charge carrier collection at each electrode.

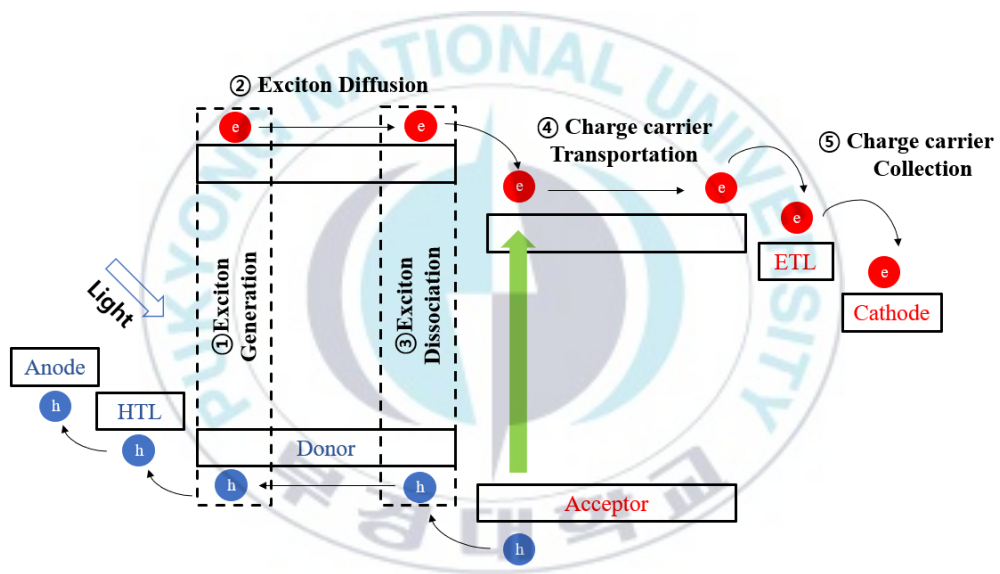


Figure I-VIIVIII. Operating principles of organic photovoltaic device

I.v General Parameters of Solar Cells

I.v.1. 1 Short-circuit Current (J_{sc})

Short-circuit current, commonly denoted as J_{sc} , means the current through the solar cell when the voltage is zero. The short-circuit current is due to the generation and collection of photogenerated carriers. For an ideal solar cell with the most appropriate resistive loss mechanism¹⁴, the short-circuit current and the photogenerated current are the same. Therefore, the short-circuit current is the maximum value of the current that can be formed in the solar cells. And several factors affect the short-circuit current. it is related to the area of solar cells. The short-circuit current density is generally used instead of short-circuit current [J_{sc} : mA/cm²].

I.v.1.2 Open Circuit Voltage (V_{oc})

Open circuit voltage, V_{oc} , refers to the maximum voltage the solar cell can use when the current is zero. Short-circuit current (J_{sc}) decreased with increasing bandgap and open-circuit voltage increased with increasing bandgap. Some parameters can affect V_{oc} such as donor's HOMO, acceptor's LUMO, and energy loss.

In a solar cell, Energy loss (E_{loss}) occurs because of the difference between the optical energy gap of a semiconductor (E_g) and its open-circuit voltage (eV_{oc}). For an ideal semiconductor, there is always some degree of energy loss in solar to electrical energy conversion. These parameters are : (1) imperfect absorption, (2) Carnot loss, and (3) étendue expansion. The first of these factors indicates that unabsorbed photons are limited by the cells, while the second and third factors reflect additive entropic losses due to the finite temperature of the sun and irreversibility in the direction of photon absorption versus emission¹⁵.

I.v.1.3 Fill Factor (FF)

The factor that determines the efficiency of solar cells is the Fill Factor (FF), and the FF follows the equation.

$$FF = \frac{J_{max} \times V_{max}}{J_{sc} \times V_{oc}} \quad (\text{Equation I - 1})$$

Fill Factor (FF) determines how “square” the J–V curve is and indicates how easy or difficult it is to extract the photogenerated carriers from a photovoltaic cell. (shown **figure I-5**)

The ideal value for FF is unity (100%) when the J–V curve is a rectangle. However, FF cannot reach 100%. because only a small voltage deviation from VOC (*VOC) is required to cause the current density to rise perpendicularly to the maximum value (JSC), and remain constant while the applied voltage changes from VOC to zero or even while reverse bias is applied¹⁶

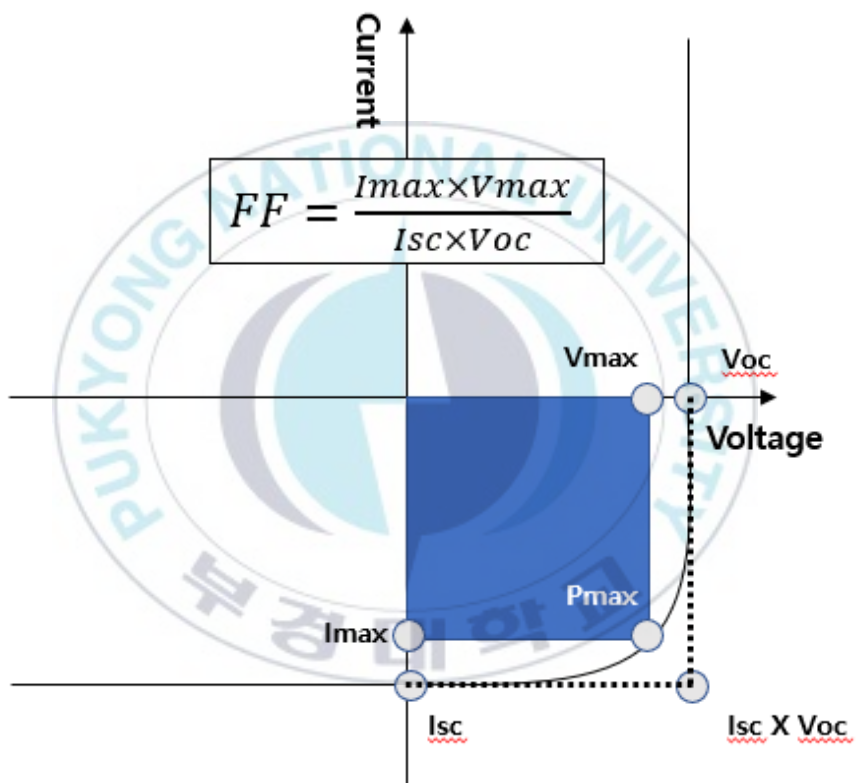


Figure IX-X. The typical current-voltage (I-V) curve of solar cells

I.v.1. 4 Power Conversion Efficiency (PCE)

Power conversion efficiency (PCE) is the most used parameter to compare the performance of solar cells with other solar cells. PCE is defined as the ratio of the energy output from the solar cell to the energy applied to the battery by the sun. In addition to reflecting the performance of the solar cell itself, efficiency depends on the spectrum and intensity of the incident light and the temperature of the solar cell. Therefore, to compare the performance of one device with that of another, it is necessary to carefully control the conditions for measuring efficiency. On the ground, solar cells are measured at AM 1.5 conditions and room temperature.

$$\eta = \frac{P_{max}}{P_{in}} = \frac{I_{max} \times V_{max}}{P_{in}} = \frac{FF \times J_{sc} \times V_{oc}}{P_{in}} \quad (\text{Equation I-2})$$

Chapter II Synthesis of 4,7-dibromo-1H-indene-1,3(2H)-dione based Conjugated polymers for Polymer Solar Cells.

II.i Introduction

Organic solar cells (OSCs) convert light energy into electricity using an energy harvesting technique, and they have several benefits including being processable in solutions, being able to be made for large area applications, and being able to be used for flexible electronics¹⁷⁻²¹. In recent years, bulk heterojunctions (BHJ) have attracted attention due to their large interfacial areas composed of active layers (including electron acceptors and electron donors), which lead to efficiency improvements and facilitate exciton dissociation near the donor-acceptor interface.²² In order to harvest efficient solar photons, we are aiming to extend the absorption in the visible region with high molar extinction/absorption coefficients. An active layer depends significantly on the alignment of donor-acceptor moiety energies. In addition, combined π -conjugated electron D-A units and their intramolecular charge-transfer (ICT) behavior support the uplifting of photo-absorption in the visible region and tune the energy levels of small molecules²³. The indandione type of core unit has recently gained attention as an electron acceptor unit due to its multiple modification sites and a strong electron-withdrawing ability as an organic moiety.²⁴⁻²⁶ Therefore, In this study, We have been successfully synthesized based on 1,3-indandione derivatives, and also introduced hexylthiophene for extending conjugation length, decreasing the HOMO level, and improving solubility^{25, 27-29},

Through the introduction of thiophene donor moiety into the benzothiazole molecule³⁰,

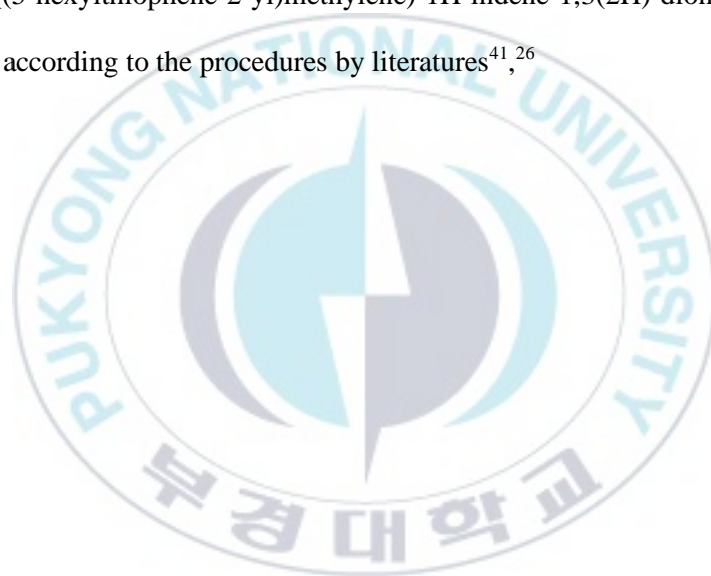
the stability, solubility, optical and electronic properties have been tremendously improved³¹. Benzodithiophene (BDT) units functionalized with long alkyl side chains were employed to ensure solution processability³²⁻³⁴, and fluorinated Benzodithiophene (BDTF) units were studied to fine-tune the donor energy levels and film morphology³⁵. We have been polymerized typical donor-acceptor (D-A) configuration where the BDT or BDTF is the donor (D) unit while the 4,7-dibromo-2-((5-hexylthiophen-2-yl)methylene)-1H-indene-1,3(2H)-dione (IND-HT) is the electron acceptor (A) unit.

There are many advantages to using fullerene acceptors such as [6,6]-phenyl C71 butyric acid methyl ester (PC₇₁BM)³⁶⁻³⁸, including high electron mobility, appropriate energy levels, and isotropic charge transport³⁹. The OSCs based on IND-HT-BDT or IND-HT-BDTF as the donor with PC₇₁BM as the acceptor were fabricated to investigate the photovoltaic properties for the application of the photoactive materials. Despite their many merits, fullerene acceptors suffer from many shortcomings, such as low absorption coefficient in the visible region, complex synthesis and purification, and high price³⁹. Non-fullerene acceptors (NFA) not only exhibit greater light absorption and widen the spectral range and energy levels, but also enable much fewer energy losses below ~0.6 eV, allowing PCE-based OSCs to perform better than those based on fullerenes⁴⁰. So, we fabricated OSCs based on IND-HT-BDT or IND-HT-BDTF as the donor with non-fullerene such as Y6BO as the acceptor and investigate the photovoltaic properties for the application of the photoactive materials.

II.ii Experimental

II.ii.1 Materials

All chemicals were purchased from Sigma-Aldrich Co, Tokyo Chemical industry (TCI) or Alfa Aesar (A Johnson Matthey Company) and used as received unless otherwise described. For 2-Hexylthiophene (2), 4,7-dibromo-1H-indene-1,3(2H)-dione (4), 4,7-dibromo-2-((5-hexylthiophene-2-yl)methylene)-1H-indene-1,3(2H)-dione (5) was synthesized according to the procedures by literatures^{41,26}



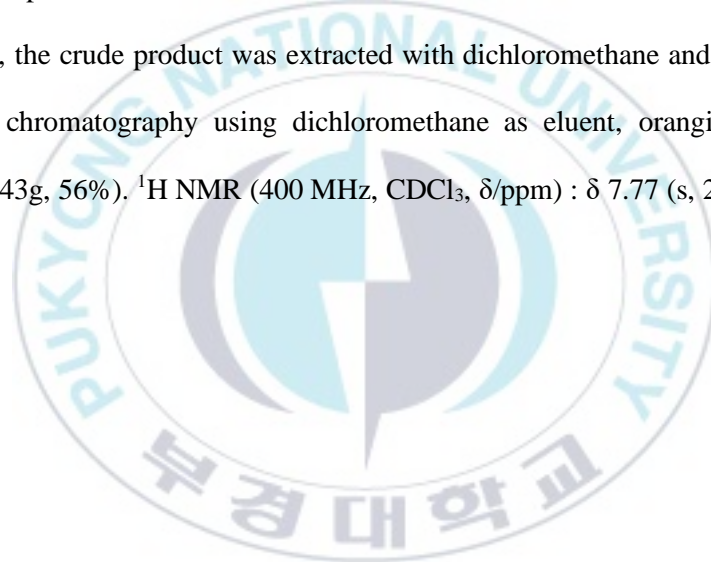
II.ii.2 Synthesis of IND-HT

5-Hexylthiophene-2-carbaldehyde (2)

Compound 2 was synthesized by the Vilsmeier reaction. Under Nitrogen atmosphere, a solution of compound 1 (1.68g, 10mmol.) was dissolved in dichloroethane (20mL). Anhydrous DMF (0.77mL, 10mmol.) was added dropwise, then POCl₃ (0.93mL, 10mmol.) was added slowly at 0 °C. The mixture was stirred at 0 °C for 20 min and then heated to 90 °C for 24 h. After cooling to room temperature, water (30 mL) was added to quench the reaction. The mixture was extracted with dichloromethane and washed with water. The organic phase was dried over anhydrous MgSO₄ and the solvent was removed by rotary evaporation. The crude product was purified on silica gel chromatography using Dichloromethane/Hexane (1/1 by volume) as eluent to afford a yellow liquid (1.22g, 62.1%). ¹H NMR (400 MHz, CDCl₃, δ/ppm) : δ 9.81 (s, 1H), δ 7.61-7.60 (d, 1H), δ 6.90-6.89 (d, 1H), δ 2.88-2.85 (t, 2H), δ 1.74-1.66 (m, 2H), δ 1.41-1.25 (m, 6H), δ 0.90-0.87(m, 3H).

4,7-dibromo-1H-indene-1,3(2H)-dione (4)

Triethylamine (3.80 g, 37.6mmol) and ethyl acetoacetate (3.67g, 28.2 mmol) were added to the solution of compound 3 (4.33 g, 9.4 mmol) in acetic anhydride (19.19 g, 188 mmol) under nitrogen. The mixture was stirred overnight at 65 °C The mixture was poured into ice-water with HCl and then extracted with dichloromethane. The organic phase was evaporated and refluxed in concentrated HCl for 1 h. After cooling to room temperature, the crude product was extracted with dichloromethane and then purified by column chromatography using dichloromethane as eluent, orangish solid was obtained (2.43g, 56%). ¹H NMR (400 MHz, CDCl₃, δ/ppm) : δ 7.77 (s, 2H), δ 3.33 (s, 2H).



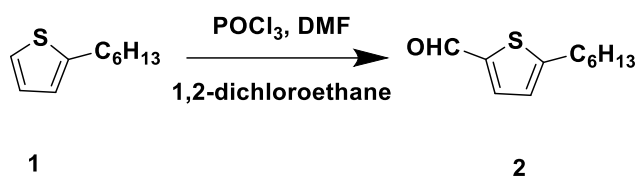
**4,7-dibromo-2-((5-hexylthiophene-2-yl)methylene)-1H-indene-
1,3(2H)-dione (5)**

In R.B flask, compound 4 (2.43g, 8mmol) and compound 2 (0.82g, 7.27mmol.) was dissolved in chloroform (10mL), and 5 drops of pyridine were added to the solution. The solution was stirred at 65 °C for overnight. After cooled to room temperature, the mixture was extracted with dichloromethane and washed with water. The organic phase was dried over anhydrous MgSO₄ and the solvent was removed by rotary evaporation. The crude product was purified on silica gel chromatography using dichloromethane as an eluent to afford a brown powder (3.04g, 79%). ¹H NMR (400 MHz, CDCl₃, δ/ppm) : δ 7.99 (s, 1H), δ 7.90-7.89 (d, 1H), δ 7.68 (s, 2H) , δ 6.99-6.98 (d, 1H), δ 2.95-2.91 (t, 2H), δ 1.80-1.72 (m, 2H), δ 1.41-1.27 (m, 8H), δ 0.90-0.86 (t, 3H).

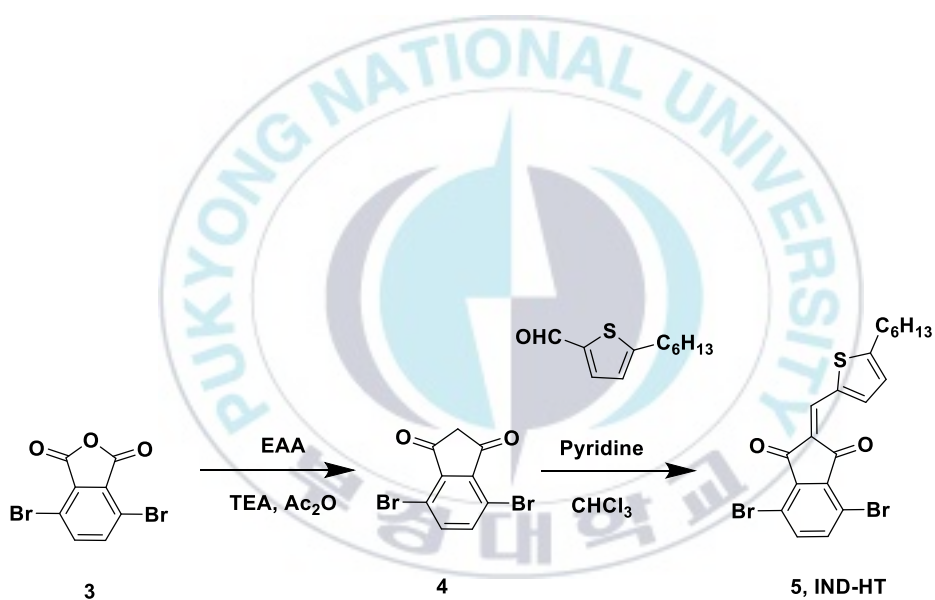
II.ii.3 Synthesis of D-A type polymers by stille coupling reaction⁴²

In a Schlenk tube, the selected monomer (BDT or BDTF) and compound 5 and Pd(PPh₃)₄ (3% mol) were mixed together in dry toluene. The solution was stirred at 90 °C for 4 hours. The polymerization was ended by adding two end-capping agents of 2-trimethylstannylthiophene and 2-bromothiophene at 1 hour interval. After that, the polymer solution was precipitated in methanol, and the polymer solid was collected by filtration. Soxhlet extraction using methanol, acetone, hexane, and chloroform was consecutively carried out to purify the polymer. The chloroform fraction was concentrated and the polymer was precipitated again in methanol. Finally, the polymer solid was dried under vacuum at 50°C.

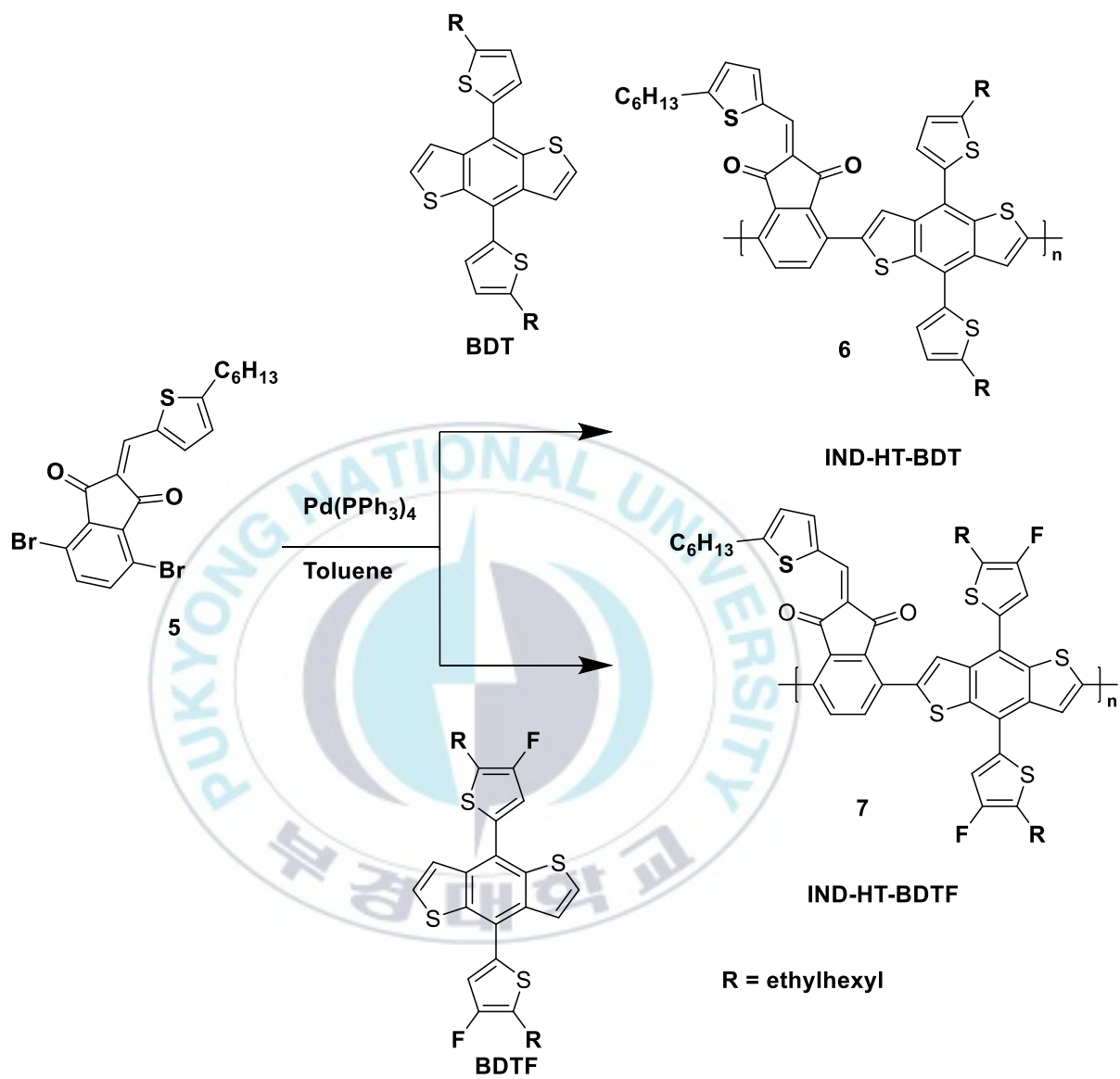
Mn (IND-HT-BDT) : 11 kDa Mn (IND-HT-BDTF) : 55 kDa



Scheme 1 Synthesis of 5-Hexylthiophene-2-carbaldehyde



Scheme 2. Synthesis of 4,7-dibromo-2-((5-hexylthiophene-2-yl)methylene)-1H-indene-1,3(2H)-dione



Scheme 3. Polymerization of IND-HT-BDT, IND-HT-BDTF.

II.ii.4 Measurement

The thickness of the ZnO and the active layer were measured using an Alpha-Step IQ surface profiler (KLA-Tencor Co.). The current density-voltage measurements were performed under simulated light (AM 1.5G, 1.0 sun condition, Peccell Technology, Model PEC-L01) from a 150 W Xe lamp, using a KEITHLEY Model 2400 source-measure unit. A calibrated Si reference cell with a KG5 filter certified by the National Institute of Advanced Industrial Science and Technology was used to confirm 1.0 sun condition. Nonmodulated impedance spectroscopy was performed using an impedance analyzer (WonATech., Zcon™ Impedance Monitor). A 50 mV voltage perturbation was applied over a constantly applied bias, 0 ~ 1.0 V, in the frequency range between 1 Hz and 1.0 MHz under the dark condition with the device for a current density - voltage (J-V) characteristics. The incident photon-to-electron conversion efficiency (IPCE) spectra were measured by a 150 W Xe lamp (Abet Technology Model LS150), monochromator (Oriel Cornerstone 130 1/8 m), and source-measure unit (KEITHLEY Model 2400). All the measurements were performed at room temperature under ambient atmosphere. Grazing-incidence wide-angle X-ray scattering (GIWAXS) spectra were obtained on the 3C beamline with 13 keV ($\lambda = 0.123$ nm) X-ray irradiation source and the beam size of 300 μm (height) \times 23 μm (width) in the Pohang Accelerator Laboratory (PAL).

II.ii.5 Fabrication of OSCs

II.ii.5. 1 polymer with fullerene acceptor (PC₇₁BM).

In the OSCs with the structure of ITO/ZnO (~25 nm)/active layer (IND-HT-BDT or IND-HT-BDTF : PC₇₁BM) (80 nm)/MoO₃ (3 nm)/Ag (100 nm) fabrication process, ITO-coated glass substrates were washed by ultrasonic agitation in detergent, deionized water, methanol, acetone, and isopropanol, respectively. The ZnO precursor was spin-cast on the pre-cleaned ITO at 4000 rpm for 1 min by using the sol-gel process⁴³. The sol-gel solution was prepared with zinc acetate dehydrate (0.100 g), and ethanolamine (0.025 mL) dissolved in 2-methoxyethanol (1 mL). The mixture was stirred at 60 °C for overnight prior to carrying out the film deposition. The thin film of ZnO precursor was annealed at 200 °C for 10 min in air. The active layer was spin-cast from a mixture of IND-HT-BDT or IND-HT-BDTF and PC₇₁BM in which the mixture was prepared to stir IND-HT-BDT or IND-HT-BDTF (6 mg) and PC₇₁BM (12 mg) in 1 mL of chlorobenzene with 3% (v/v) 1,8-diiodooctane (DIO) at 2200 and 1200 rpm for 120 s. Prior to spin coating, the active solution was filtered through a 0.2 μm membrane filter. Lastly, the MoO₃ (3 nm) and Ag (100 nm) were thermal evaporated at 2×10^{-6} Torr with a device area was 9 mm².

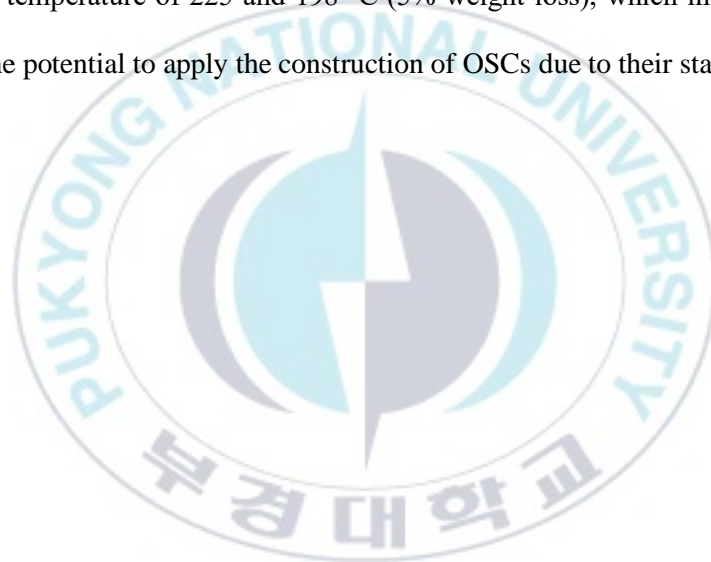
II.ii.5. 2 polymer with non-fullerene acceptor (Y6BO).

In the OSCs with the structure of ITO/ZnO (~25 nm)/active layer (IND-HT-BDT or IND-HT-BDTE:Y6BO) (85 nm)/MoO₃ (3 nm)/Ag (100 nm) fabrication process, ITO-coated glass substrates were washed by ultrasonic agitation in detergent, deionized water, methanol, acetone, and isopropanol, respectively. The ZnO precursor was spin-cast on the pre-cleaned ITO at 4000 rpm for 1 min by using the sol-gel process⁴³. The sol-gel solution was prepared with zinc acetate dehydrate (0.100 g), and ethanolamine (0.025 mL) dissolved in 2-methoxyethanol (1 mL). The mixture was stirred at 60 °C overnight prior to carrying out the film deposition. The thin film of ZnO precursor was annealed at 200 °C for 10 min in air. The active layer was spin-cast from a mixture of IND-HT-BDT or IND-HT-BDTE and Y6BO in which the mixture was prepared to stir IND-HT-BDT or IND-HT-BDTE (6 mg) and Y6BO (8 mg) in 1 mL of chloroform with 0.5% (v/v) 1-chloronaphthalene (CN) at 3000 and 2600 rpm for 60 s. Prior to spin coating, the active solution was filtered through a 0.2 μm membrane filter. This film was preheated at 110 °C for 10min in N₂. Lastly, the MoO₃ (3 nm) and Ag (100 nm) were thermal evaporated at 2×10^{-6} Torr with a device area was 9 mm².

II.iii Results and discussion

II.iii.1 Thermal analysis

The thermal properties of both polymers were investigated by using thermal gravimetric analysis (TGA) under an N₂ atmosphere at a heating rate of 10 °C min⁻¹. As shown in Figure II-1, IND-HT-BDT and IND-HT-BDTF showed a high degradation temperature of 225 and 198 °C (5% weight loss), which indicates that they have the potential to apply the construction of OSCs due to their stability.



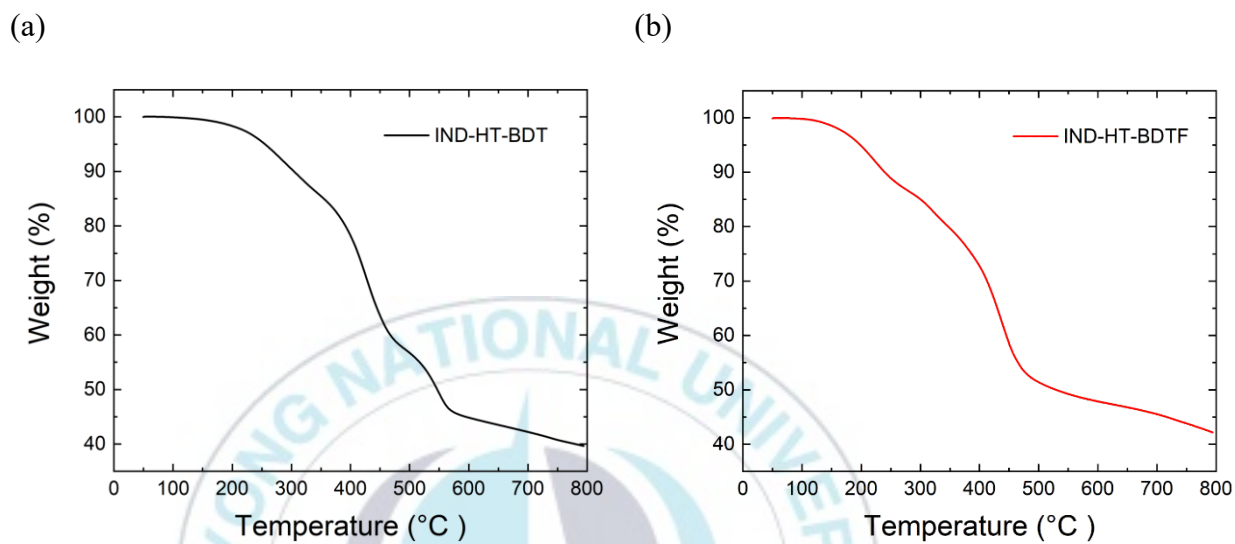


Figure II-XI. Thermal gravimetric analysis (TGA) curves of (a) IND-HT-BDT and (b) IND-HT-BDTF.

II.iii.2 Optical and Electrochemical properties.

The UV-visible spectra of both donors exhibit broad absorption in the visible region both as a solid thin film (**Figure II -2** (a)) and in the diluted CF solution (**Figure II -2** (b)). The absorption peaks of the IND-HT-BDT films are 422 and 584 nm and that of the HT-IND-BDTF films are 427, 595nm, respectively. Both polymer donors can harvest the short wavelength region from 380nm to 650nm. Compared to IND-HT-BDT, IND-HT-BDTF is red-shifted in both films and solutions because it has strong intramolecular charge transfer (ICT) stemming from fluorine groups in electron-withdrawing moiety. The optical band gaps of IND-HT-BDT and IND-HT-BDTF are 1.86V.

The energy levels of donor polymers are estimated from the onset of cyclic voltammogram (**Figure II-2** (c) and (d)). The highest occupied molecular orbital (HOMO) and lowest unoccupied molecular orbital (LUMO) energy levels of IND-HT-BDT and IND-HT-BDTF are -5.04/-3.60 eV and -5.05/-3.53 eV, respectively. As shown in energy diagram (**Figure II-2** (e)). The results are summarized in **Table II-1**.

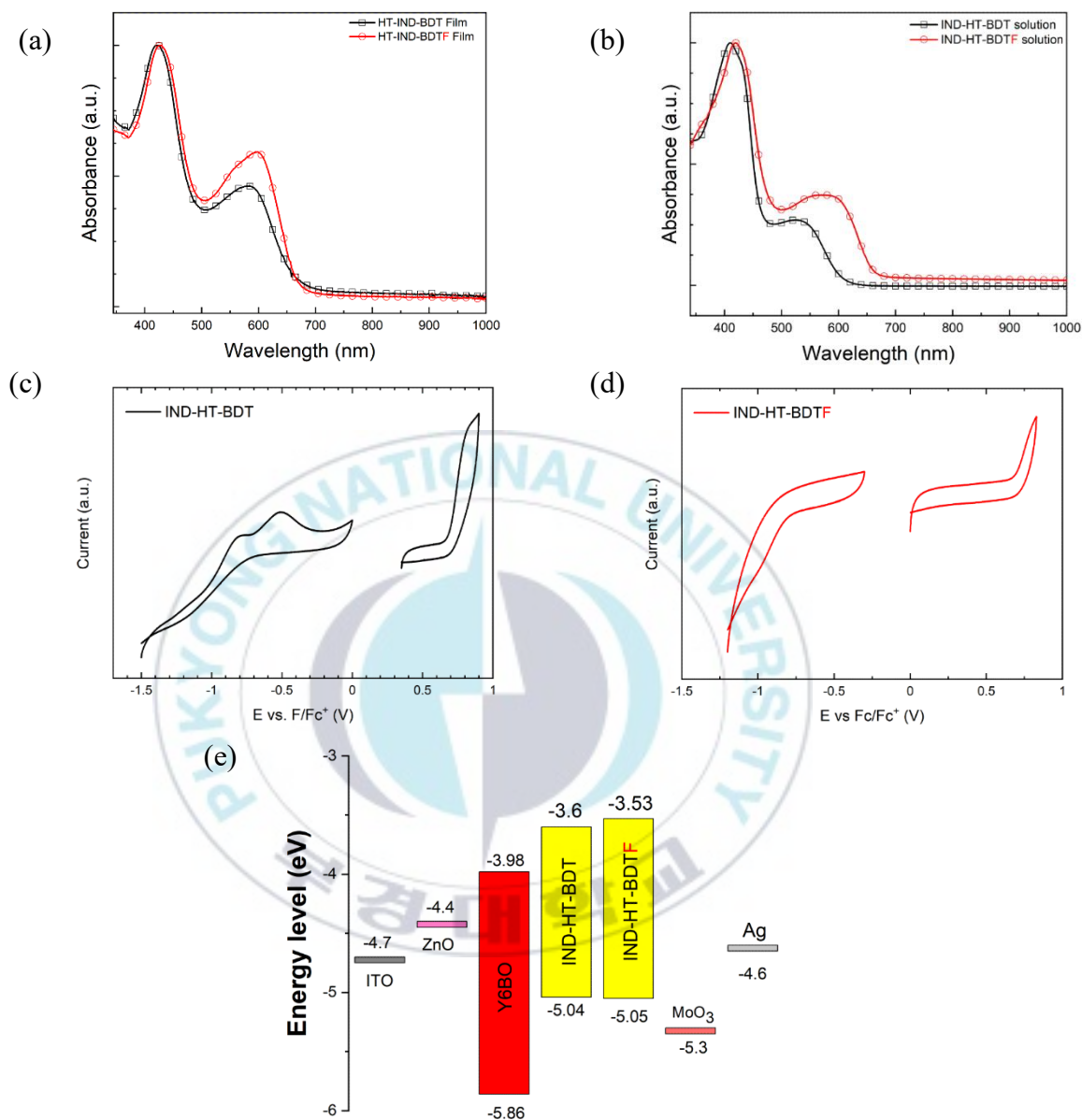


Figure II-XII. UV-visible spectra of polymer donors (a) thin films on glass substrates and (b) solution in chloroform and Cyclic voltammograms of (c) IND-HT-BDT, (d) IND-HT-BDTF and corresponding (e) energy diagram.

Table I Summary of optical and electrochemical properties of the polymer.

	λ_{edge} (nm) ^a	$\lambda_{max}^{solution}$ (nm)	HOMO (eV) ^c	LUMO (eV) ^d
	E_{gap}^{opt} (eV) ^b	λ_{max}^{film} (nm)		
IND-HT-IND	666	410, 524	-5.04	-3.60
	1.86	422, 584		
IND-HT-BDTF	668	420, 570	-5.05	-3.53
	1.86	427, 595		

^a Absorption edge of the film.

^b Estimated from the λ_{edge}

^c Maximum wavelength of the film.

^d Estimated from the oxidation onset potential

II.iii.3 Photovoltaic properties.

The inverted type devices based on ITO/ZnO/donor : PC₇₁BM/MoO₃/Ag were fabricated to investigate the photovoltaic properties of IND-HT-BDT and IND-HT-BDTF. The optimized condition of devices under AM 1.5G illumination are estimated as 3:6 (w/w) with 3% (v/v) diiodooctane (DIO) (IND-HT-BDT or IND-HT-BDTF). The J-V plots of both devices are shown in **Figure II-3** (a) and the results are summarized in **Table II-2**.

The device based on IND-HT-BDT : PC₇₁BM device exhibit a J_{sc} of 5.23 mA/cm², a V_{oc} of 0.87 V, a Fill Factor (FF) of 36.8%, and a PCE of 1.59%. In case of IND-HT-BDTF : PC₇₁BM device, it shows a J_{sc} of 5.83 mA/cm², a V_{oc} of 0.90 V, a FF of 40.3%, and a PCE of 2.10%. Despite of the F atoms, IND-HT-BDTF has stronger intramolecular charge transfer (ICT)⁴⁴, so based on IND-HT-BDTF device got higher electron mobility and J_{sc}. The series resistance (R_s) was obtained from the J-V curves obtained under 1.0 sun condition (Shown in **Table II-2**)⁴⁵. The series resistance (R_s) followed the tendency of the photovoltaic performances, which are shown in **Table II - 2**. Incident photon to current efficiency (IPCE) curves (**Figure II-2**) of the devices showed good agreement with the short-circuit current density (J_{sc}) and the performances of the devices (PCE).

PC₇₁BM has deeper LUMO levels compared with non-fullerene, so based on PC₇₁BM device can get high V_{oc}, but PC₇₁BM has many disadvantages such as its hard to tune, having a low absorption wavelength.

To overcome fullerene disadvantage, we fabricated devices based on non-fullerene devices such as Y6BO, which is the easy tune, electron-withdrawing group, and also having wider absorption wavelength. The inverted type devices based on ITO/ZnO/donor : Y6BO/MoO₃/Ag was fabricated to investigate the photovoltaic properties of IND-HT-BDT and IND-HT-BDTF. The optimized condition of devices under AM 1.5G illumination are estimated as 3:4 (w/w) with 0.5% (v/v) 1-chloronaphthelene (CN) (IND-HT-BDT or IND-HT-BDTF). The J-V plots of both devices are shown in **Figure II-3** (b) and the results are summarized in **Table II-2**.

The device based on IND-HT-BDT : Y6BO device exhibit a J_{sc} of 12.60 mA/cm², a V_{oc} of 0.65 V, a Fill Factor (FF) of 46.70%, and a PCE of 3.88%. In case of IND-HT-BDTF : Y6BO device, it shows a J_{sc} of 13.54 mA/cm², a V_{oc} of 0.82 V, a FF of 59.10%, and a PCE of 6.43%. Despite decrease of donor's HOMO with acceptor's LUMO, devices based on Y6BO decreased V_{oc}. However, The electron-withdrawing group (F and Y6BO) made a stronger dipole moment, it makes higher J_{sc} compare with devices based on PC₇₁BM as acceptor. The series resistance (R_s) was obtained from the J-V curves obtained under 1.0 sun condition (Shown in **Table II-2**)⁴⁵. The series resistance (R_s) followed the tendency of the photovoltaic performances, which are shown in **Table II - 2**. Incident photon to current efficiency (IPCE) curves (**Figure II-2**) of the devices showed good agreement with the short-circuit current density (J_{sc}) and the performances of the devices (PCE).

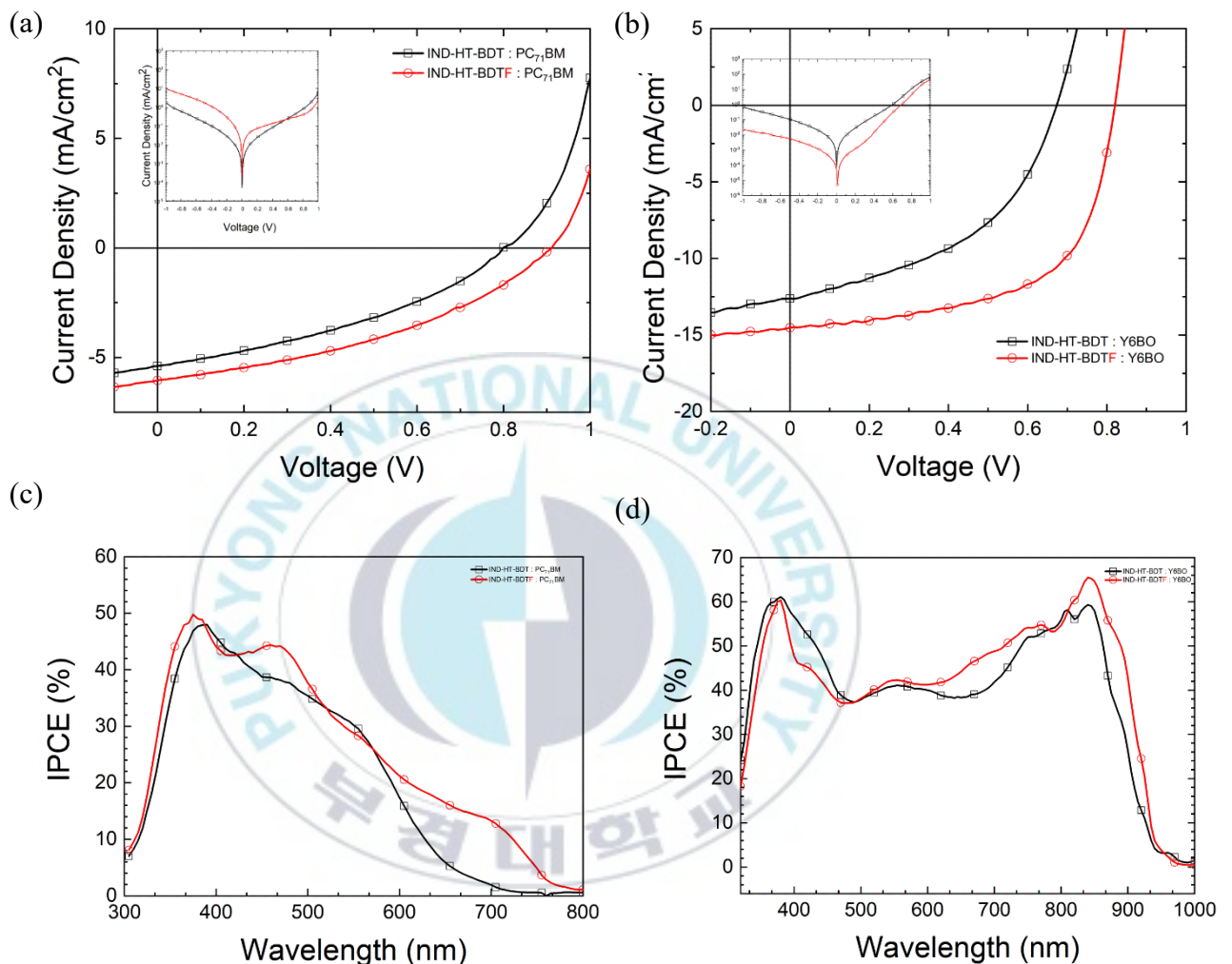


Figure II-XIII. Current density vs. voltage curves of PSCs under 1.0 sun and dark condition on the PC71BM acceptor under optimum conditions and (b) Current density vs. voltage curves of PSCs under 1.0 sun and dark condition on the Y6BO acceptor under optimum conditions. (c) the corresponding incident photon-to-current efficiency (IPCE) curves of the OSCs based on polymer donors with PC71BM. (d) the corresponding incident photon-to-current efficiency (IPCE) curves of the OSCs based on polymer donors with Y6BO.

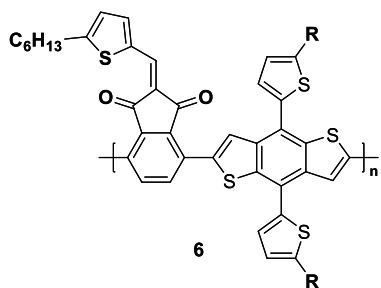
Table II The best photovoltaic parameters of the PSCs. The averages for the photovoltaic parameters of each device are given in parentheses

polymer	J_{sc} (mA/cm ²)	V_{oc} (V)	FF (%)	PCE (%)	R_s (Ω cm ²) ^b
IND-HT-BDT :	5.23	0.87	36.8	1.59	5.58
PC ₇₁ BM	(5.18)	(0.86)	(36.20)	(1.56)	
IND-HT-BDTF :	5.83	0.90	40.3	2.10	3.33
PC ₇₁ BM	(5.80)	(0.89)	(40.00)	(2.05)	
IND-HT-BDT :	12.60	0.65	46.70	3.88	2.40
Y6BO	(12.67)	(0.65)	(45.97)	(3.82)	
IND-HT-BDTF :	13.54	0.82	59.10	6.43	1.87
Y6BO	(13.21)	(0.82)	(59.22)	(6.38)	

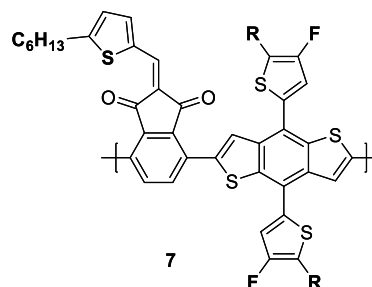
^aThe averages for photovoltaic parameters of each device are given in parentheses with mean variation. ^bSeries resistance (estimated from the device with best PCE value).

II.iii.4 Computational calculation

Computational calculations based on density functional theory (DFT) were employed to explore the electronic distribution and backbone conformation. The DFT calculations were performed using Gaussian 09 software with the hybrid B3LYP correlation functional and split valence 6-31G(d) basis set.⁴⁶ The electronic distributions and optimized geometries of polymer donors are depicted in Figure II-3. The HOMO orbitals are delocalized in the donor part (BDT or BDTF) in donor polymer. On the other hand, the LUMO orbitals are localized in the acceptor part (IND-HT) in donor polymer. (Figure II-3). The optimized geometry of IND-HT-BDT and IND-HT-BDTF are -5.04/-3.60 and -5.05/-3.53 eV, respectively.

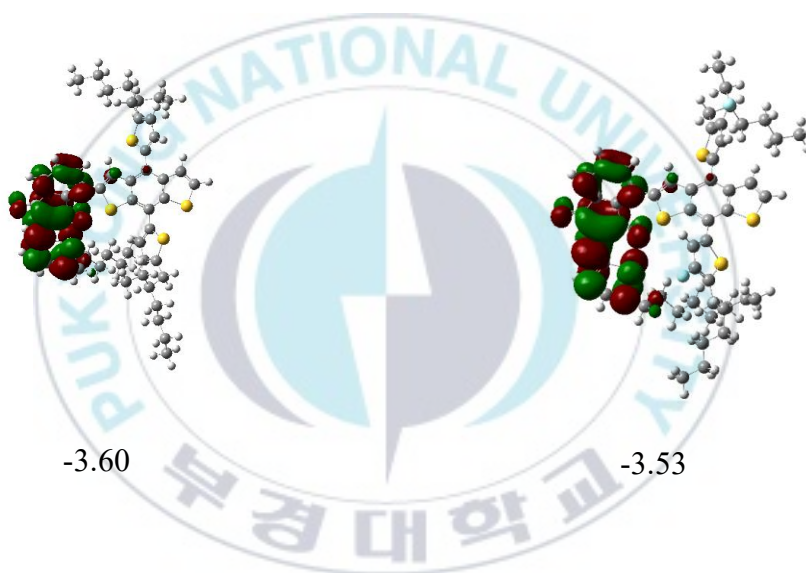


6
IND-HT-BDT



7
IND-HT-BDTF

LUMO



HOMO



Figure II-IV The electronic distributions of polymer donors obtained from density functional theory (DFT) calculations

II.iv Morphology of the polymers and their blends

An active layer's molecular ordering and crystallinity are crucial for determining the overall performance of a PSC. Thus, GIWAXS measurements⁴⁷ were conducted on the neat polymer films and on their blend films with either a PC₇₁BM or Y6BO acceptor, and the resultant images and plots are shown in **Figure II-6**. The corresponding intensity profiles in the out-of-plane (OOP) and in-plane (IP) directions are presented in **Figure II-5** and summarized in **Table II-3, Table II-4**.

According to the GIWAXS patterns (**Figure II-6 (a), (b)**) and scattering profiles (**Figure II-5**), all neat polymer films showed clear (100) and (010) peaks in the IP and OOP directions, respectively. It is typical for polymer chains to be oriented face-on to the surface with enhanced crystallinity.^{48,49} The positions of the π - π stacking peaks of IND-HT -BDT (1.289 Å⁻¹), IND-HT-BDT: PC₇₁BM (1.850 Å⁻¹), IND-HT-BDT: Y6BO (1.351 Å⁻¹) in the OOP direction were equivalent to the π - π stacking distances of 4.87, 3.39, 4.65 Å, respectively. The smaller π - π stacking distance in the face-on crystalline domain was advantageous for enhancing the photovoltaic properties of the polymers because the charge transfer in the favorable vertical direction was readily facilitated. So blended polymer films with PC₇₁BM, and Y6BO enhanced face on orientation in the OOP direction. The positions of the π - π stacking peaks of IND-HT-BDT (1.498 Å⁻¹), IND-HT-BDT: PC₇₁BM (1.886 Å⁻¹), IND-HT-BDT: Y6BO (1.514 Å⁻¹) in the IP direction were equivalent to the π - π stacking distances of 4.19, 3.33, 4.15 Å, respectively. IP direction parts also blended polymer with PC₇₁BM strongly enhanced the π - π stacking, Y6BO case enhanced slightly enhanced^{50,51}. the good miscibility between the polymers and PC₇₁BM, Y6BO can result in a favorable face-on orientation

in the blended film.

The positions of the π - π stacking peaks of IND-HT-BDTF (1.0114 \AA^{-1}), IND-HT-BDT: PC₇₁BM (1.835 \AA^{-1}), IND-HT-BDT: Y6BO ($1.387, 1.691 \text{ \AA}^{-1}$) in the OOP direction were equivalent to the π - π stacking distances of 6.21, 3.42, 4.53, 3.71 \AA , respectively. Blended polymer films with PC₇₁BM, and Y6BO enhanced face on orientation in the OOP direction. The positions of the π - π stacking peaks of IND-HT-BDT (1.949 \AA^{-1}), IND-HT-BDT: PC₇₁BM (0.937 \AA^{-1}), IND-HT-BDT: Y6BO ($1.558, 1.851 \text{ \AA}^{-1}$) in the IP direction were equivalent to the π - π stacking distances of 3.22, 6.70, 4.03, 3.39 \AA , respectively. IP direction parts decreased the distances, But OOT direction enhancing face-on direction ordering. Interestingly, After Blended polymer films with Y6BO, peaks of IN, OOP divided more over 1 peak. That is because blend films with Y6BO demonstrate microstructural features of its individual components⁵².

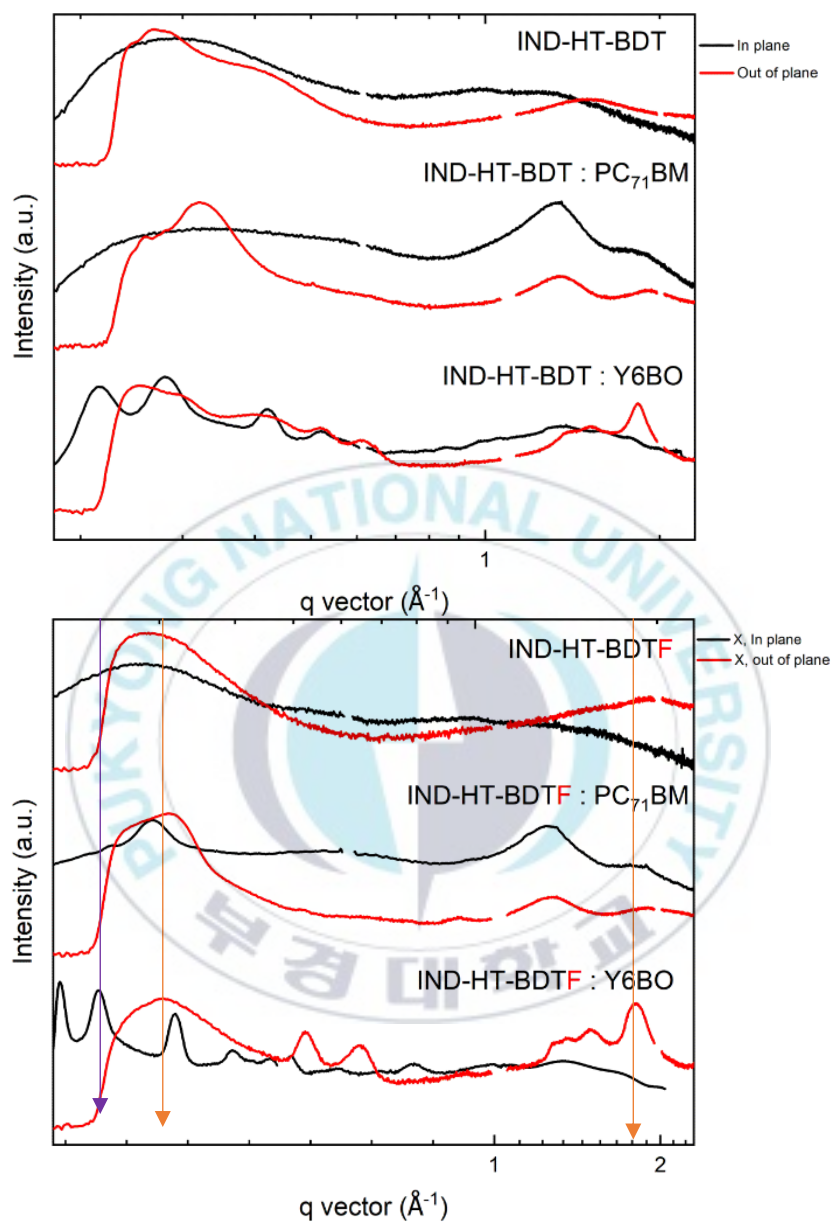


Figure II-V GIWAXS intensity profiles along the in-plane (black line) and out-of-plane (red line) directions. The in-plane and out-of-plane from PC71BM (blue line), The in-plane of Y6BO (purple line), out-of-plane of Y6BO (orange line).

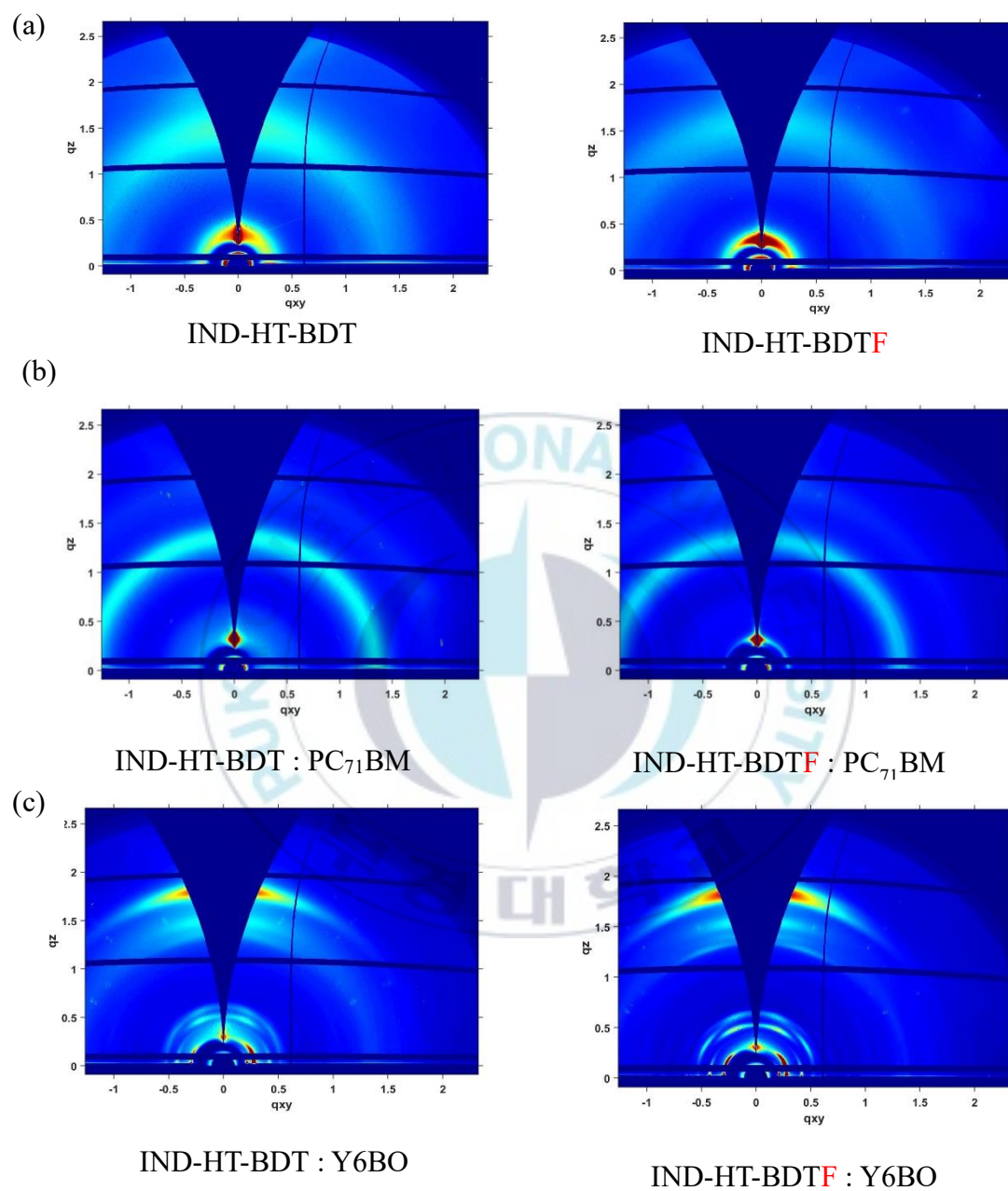


Figure II-XIVI GIWAXS images of (a) neat IND-HT-BDT, IND-HT-BDTF, (b) polymer with PC71BM optimized blend film, and (c) polymer with Y6BO optimized blend film.

Table III The corresponding line cut in in-plane (IP) and out-of-plane (OOP) directions of neat polymers, blend films with PC₇₁BM, and blend films with Y6BO.

	Polymer π - π In plane / out of plane	Polymer lamella In plane / out of plane
HT-IND-BDT	1.289 (0.487 nm) / 1.498 (0.419 nm)	0.300, 0.977 (2.095, 0.673 nm) / 0.268, 0.382 (2.347, 1.646 nm)
HT-IND-BDT : PC ₇₁ BM	1.850 (0.339 nm) / 1.886 (0.333 nm)	0.336 (1.866 nm) / 0.258, 0.317 (2.431, 1.981 nm)
HT-IND-BDT : Y6BO	1.351 (0.465 nm) / 1.514 (0.415 nm)	0.421, 0.521 (1.491, 1.205 nm) / 0.284, 0.404, 0.519, 0.608 (2.211, 1.554, 1.210, 1.033 nm)
PC ₇₁ BM	1.332 (0.471 nm) / 1.347 (0.466 nm)	X / X
Y6BO	X / 1.834 (0.342 nm)	0.215, 0.279 (2.921, 2.251 nm) / 0.253 (2.482 nm)

Table IV The corresponding line cut in in-plane (IP) and out-of-plane (OOP) directions of neat polymers, blend films with PC₇₁BM, and blend films with Y6BO.

	Polymer π - π In plane / out of plane	Polymer lamella In plane / out of plane
HT-IND-BDTF	1.0114 (0.621 nm) / 1.949 (0.322 nm)	0.279 (2.255 nm) / 0.288 (2.182 nm)
HT-IND-BDTF : PC₇₁BM	1.835 (0.342 nm) / 0.937 (0.670 nm)	0.292 (2.148 nm) / 0.312, (2.013 nm)
HT-IND-BDTF : Y6BO	1.387, 1.691 (0.453, 0.371 nm) / 1.558, 1.851 (0.403, 0.339 nm)	0.422, 0.526, 0.855 (1.488, 1.194, 0.735 nm) / 0.523, 0.646 (1.201, 0.972 nm)
PC₇₁BM	1.311 (0.479 nm) / 1.364 (0.460 nm)	X / X
Y6BO	X / 1.911 (0.329 nm)	0.212, 0.282 (2.962, 2.227 nm) / 0.304 (2.066 nm)

II.v Conclusion

In this work, conjugated donor materials based on Indandione with BDT or BDTF, named IND-HT-BDT, IND-HT-BDTF were designed and synthesized for organic solar cells. The hexyl-thiophene as an electron-donating group, when combined with IND, can effectively form a powerful push-pull structure that induces effective ICT and enhanced optical absorption. The PCEs of the devices based on polymer donors with BDTF were better. Furthermore, the devices with fullerene acceptor were fabricated, the PCEs were not good. However, polymer donors with non-fullerene enhanced push-pull structure and show a broad light absorption range as well as good solubility. After being added to CN, the PCE of IND-HT-BDTF:Y6BO based device was greatly improved up to 6.43%.

Chapter III Effect of Dihexyl-thiophene with 4,7-dibromo-1H-indene-1,3(2H)-dione based Conjugated polymers as donor for Polymer Solar Cells.

III.i Introduction

In recent years, polymer solar cells (PSCs) that rely on n-type organic semiconductors have been gaining attention as solar cell technology. Compared to conventional fullerene acceptors, n type organic semiconductor (n-OS) acceptors have unique advantages, such as crystallinity and optical absorption, materials selections and low cost production^{53, 54, 55, 56}. So far, by fine chemical modification and reasonable matching of high-performance acceptor and donor materials^{56, 57}. Therefore, in this study, we have been successfully synthesized based on 1,3-indandione derivatives, and also introduced dihexyl-thiophene for extending conjugation length, decreasing the HOMO level, and higher solubility.

Through the introduction of thiophene donor moiety into the benzothiazole molecule, the stability, solubility, optical and electronic properties have been tremendously improved³¹. Benzodithiophene (BDT) units functionalized with long alkyl side chains were employed to ensure solution processability, and fluorinated Benzodithiophene (BDTF) units were studied to fine-tune the donor energy levels and film morphology³⁵. We have been polymerized typical donor-acceptor (D-A) configuration where the BDT or BDTF is the donor (D) unit while the 4,7-dibromo-2-((4,5-dihexylthiophen-2-yl)methylene)-1H-indene-1,3(2H)-dione (IND-DHT) is the electron acceptor (A) unit.

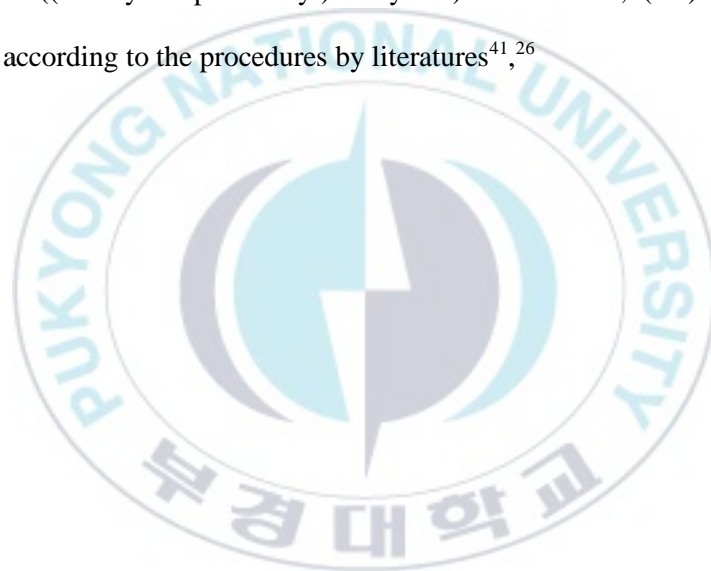
Non-fullerene acceptors (NFA) not only exhibit greater light absorption and widen the spectral range and energy levels, but also enable much fewer energy losses below ~ 0.6 eV, allowing PCE-based OSCs to perform better than those based on fullerenes⁴⁰. So, we fabricated OSCs based on IND-DHT-BDT or IND-DHT-BDTF as the donor with non-fullerene such as Y6BO as the acceptor and investigate the photovoltaic properties for the application of the photoactive materials.



III.ii Experimental

III.ii.1 Materials

All chemicals were purchased from Sigma-Aldrich Co, Tokyo Chemical industry (TCI) or Alfa Aesar (A Johnson Matthey Company) and used as received unless otherwise described. For 2,3-Dihexylthiophene (2), 4,7-dibromo-1H-indene-1,3(2H)-dione (4), 4,7-dibromo-2-((5-hexylthiophene-2-yl)methylene)-1H-indene-1,3(2H)-dione (5) was synthesized according to the procedures by literatures^{41,26}



III.ii.2 Synthesis of IND-DHT

Synthesis of 2-Bromo-3-hexylthiophene (4).

After 3 g (17.8 mmol) of 3-hexylthiophene was dissolved in 40 mL of tetrahydrofuran (THF), 3.49 g (19.6 mmol) of N-bromosuccinimide (NBS) was slowly added under ice-bath condition. The reaction was kept for 3 hours at room temperature and monitored by TLC. The reaction was ended by adding 100 mL of water and then the mixture was extracted with 100 mL of diethyl ether. The organic phase was collected and washed several times with brine. After dried over MgSO₄, the solvent was evaporated under reduced pressure. Finally, the product was purified by column chromatography using hexane as eluent, transparent oil was obtained (4.10 g, 93.4 %). MS: [M⁺], m/z 246. ¹H NMR (400 MHz, CDCl₃, ppm): δ 7.20 (d, 1H), 6.82 (d, 1H), 2.60 (t, 2H), 1.61 (m, 2H), 1.35 (m, 6H), 0.93 (t, 3H).

Synthesis of 2,3-dehexylthiophene (5)

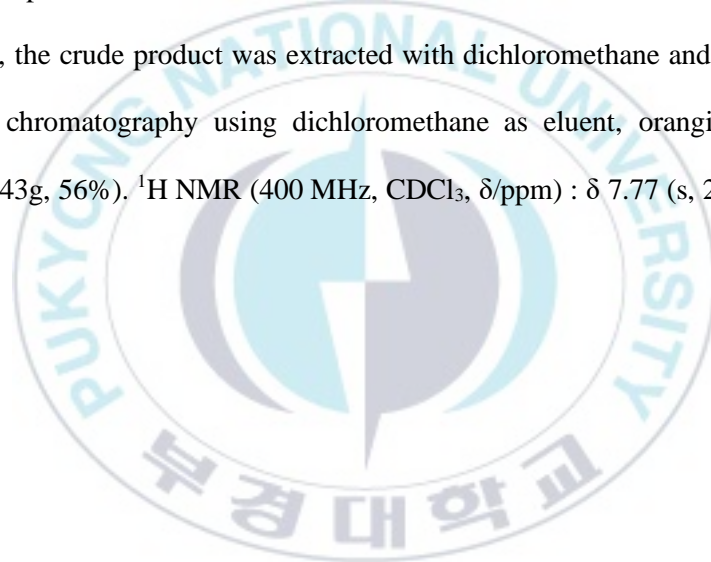
In a two-necked flask, 5.41 g (21.9 mmol) of 2-bromo-3-hexylthiophene and 0.59 g (1 mmol) of Ni(dppp)Cl₂ were dissolved in 25 mL of distilled THF. Under ice-bath condition, hexyl-MgBr was slowly added into the reaction mixture. Then the mixture was refluxed under nitrogen condition overnight. Saturated solution of ammonium chloride was added to end the reaction and the reaction mixture was further extracted with hexane. After washing several times with brine, the mixture was dried over MgSO₄ and the solvent was evaporated by rotary evaporator. The product was purified by column chromatography using hexane as eluent, yellow oil was obtained. (4.90 g, 88.0 %). ¹H NMR (400 MHz, CDCl₃, ppm): δ 7.03 (d, 1H), 6.82 (d, 1H), 2.72 (t, 2H), 2.51 (t, 2H), 1.63 (m, 2H), 1.55 (m, 2H), 1.31 (m, 12H), 0.90 (t, 6H).

Synthesis of 4,5-dehexylthiophene-2-carbaldehyde (6)

A mixture of DMF 6.95 g (95.1 mmol) and POCl₃ 14.58 g (95.1 mmol) was stirred at 0°C for 30 minutes to form the Vilsmeier reagent; the Vilsmeier reagent was slowly added to a solution of 6.15 g (24.4 mmol) of 2,3-dihexylthiophene in 48 mL of dichloroethane. The reaction mixture was refluxed overnight under N₂ environment. After cooling down to room temperature, aqueous NaHCO₃ solution was added. The mixture was extracted with MC, dried over with MgSO₄ and the solvent was evaporated by reduced pressure. A brown oil was further purified by silica gel column chromatography using MC / hexane (6:4) to afford product as yellow oil (6.60 g, 96.0 %). MS: [M⁺], m/z 280. ¹H NMR (400 MHz, CDCl₃, ppm): δ 9.78 (s, 1H), 7.03 (s, 1H), 2.77 (t, 2H), 2.52 (t, 2H), 1.66 (m, 2H), 1.57 (m, 2H), 1.31 (m, 12H), 0.89 (t, 6H).

4,7-dibromo-1H-indene-1,3(2H)-dione (8)

Triethylamine (3.80 g, 37.6mmol) and ethyl acetoacetate (3.67g, 28.2 mmol) were added to the solution of compound 7 (4.33 g, 9.4 mmol) in acetic anhydride (19.19 g, 188 mmol) under nitrogen. The mixture was stirred overnight at 65 °C The mixture was poured into ice-water with HCl and then extracted with dichloromethane. The organic phase was evaporated and refluxed in concentrated HCl for 1 h. After cooling to room temperature, the crude product was extracted with dichloromethane and then purified by column chromatography using dichloromethane as eluent, orangish solid was obtained (2.43g, 56%). ¹H NMR (400 MHz, CDCl₃, δ/ppm) : δ 7.77 (s, 2H), δ 3.33 (s, 2H).

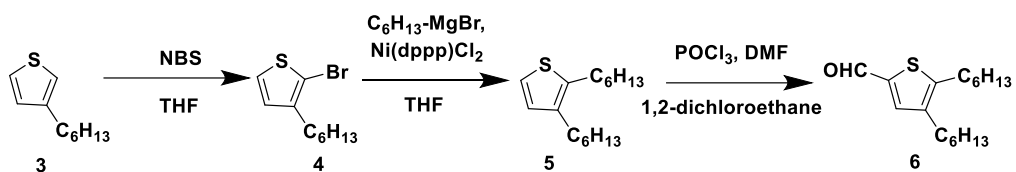


**4,7-dibromo-2-((4,5-Dihexylthiophene-2-yl)methylene)-1H-indene-
1,3(2H)-dione (9)**

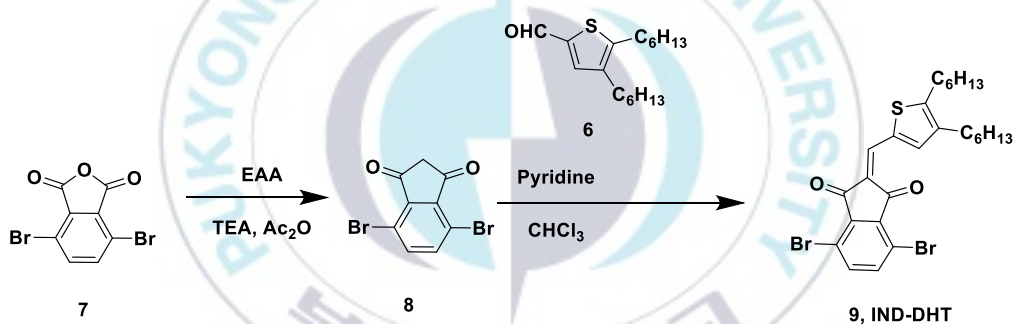
In R.B flask, compound 8 (2.43g, 8mmol) and compound 6 (2.04g, 7.27mmol.) was dissolved in chloroform (10mL), and 5 drops of pyridine were added to the solution. The solution was stirred at 65 °C for overnight. After cooled to room temperature, the mixture was extracted with dichloromethane and washed with water. The organic phase was dried over anhydrous MgSO₄, and the solvent was removed by rotary evaporation. The crude product was purified on silica gel chromatography using dichloromethane as an eluent to afford a brown powder (3.04g, 79%). ¹H NMR (400 MHz, CDCl₃, δ/ppm) δ 7.97 (s, 1H), δ 7.82 (s, 1H), δ 7.69 (2, 2H), δ 2.88-2.84 (t, 2H), δ 2.59-2.55 (t, 2H), δ 1.78-1.71 (m, 2H), δ 1.65-1.58 (m, 2H), δ 1.46-1.26 (m, 12H), δ 0.93-0.89 (m, 6H).

III.ii.3 polymerization of D-A type polymers by stille coupling reaction⁴²

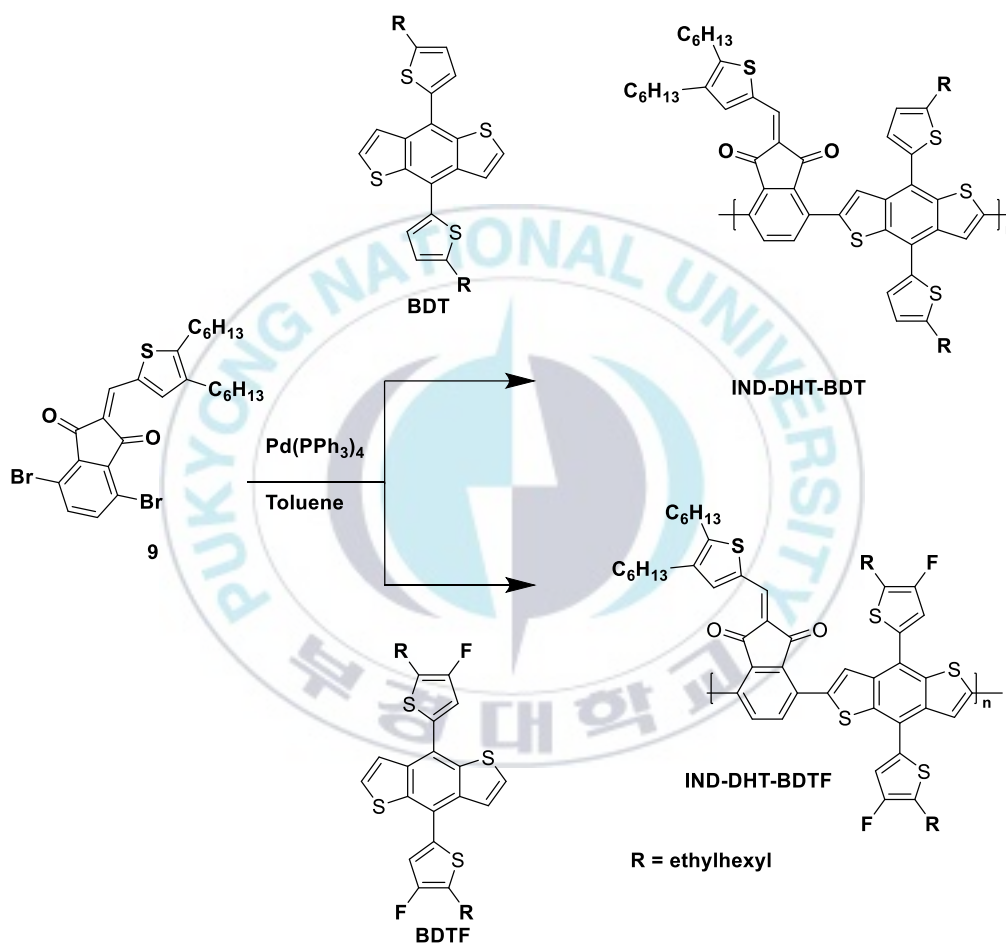
In a Schlenk tube, the selected monomer (BDT or BDTF) and compound 9 and Pd(PPh₃)₄ (3% mol) were mixed together in dry toluene. The solution was stirred at 90 °C for 4 hours. The polymerization was ended by adding two end-capping agents of 2-trimethylstannylthiophene and 2-bromothiophene at 1 hour interval. After that, the polymer solution was precipitated in methanol, and the polymer solid was collected by filtration. Soxhlet extraction using methanol, acetone, hexane, and chloroform was consecutively carried out to purify the polymer. The chloroform fraction was concentrated, and the polymer was precipitated again in methanol. Finally, the polymer solid was dried under vacuum at 50°C.



Scheme 4 Synthesis of 4,5-Dihexylthiophene-2-carbaldehyde



Scheme 5 Synthesis of 4,7-dibromo-2-((4,5-Dihexylthiophene-2-yl)methylene)-1H-indene-1,3(2H)-dione



Scheme 6 Polymerization of IND-DHT-BDT, IND-DHT-BDTF

III.ii.4 Measurement

The thickness of the ZnO and the active layer were measured using an Alpha-Step IQ surface profiler (KLA-Tencor Co.). The current density-voltage measurements were performed under simulated light (AM 1.5G, 1.0 sun condition, Peccell Technology, Model PEC-L01) from a 150 W Xe lamp, using a KEITHLEY Model 2400 source-measure unit. A calibrated Si reference cell with a KG5 filter certified by the National Institute of Advanced Industrial Science and Technology was used to confirm 1.0 sun condition. Non-modulated impedance spectroscopy was performed using an impedance analyzer (WonATech., ZconTM Impedance Monitor). A 50 mV voltage perturbation was applied over a constantly applied bias, 0 ~ 1.0 V, in the frequency range between 1 Hz and 1.0 MHz under the dark condition with the device for a current density - voltage (J-V) characteristics. The incident photon-to-electron conversion efficiency (IPCE) spectra were measured by a 150 W Xe lamp (Abet Technology Model LS150), monochromator (Oriel Cornerstone 130 1/8 m), and source-measure unit (KEITHLEY Model 2400). All the measurements were performed at room temperature under ambient atmosphere. Grazing-incidence wide-angle X-ray scattering (GIWAXS) spectra were obtained on the 3C beamline with 13 keV ($\lambda = 0.123$ nm) X-ray irradiation source and the beam size of 300 μm (height) \times 23 μm (width) in the Pohang Accelerator Laboratory (PAL).

polymer with non-fullerene acceptor (Y6BO).

In the OSCs with the structure of ITO/ZnO (~25 nm)/active layer (IND-DHT-BDT or IND-DHT-BDTF:Y6BO) (75 nm)/MoO₃ (3 nm)/Ag (100 nm) fabrication process, ITO-coated glass substrates were washed by ultrasonic agitation in detergent, deionized water, methanol, acetone, and isopropanol, respectively. The ZnO precursor was spin-cast on the pre-cleaned ITO at 4000 rpm for 1 min by using the sol-gel process⁴³. The sol-gel solution was prepared with zinc acetate dehydrate (0.100 g), and ethanolamine (0.025 mL) dissolved in 2-methoxyethanol (1 mL). The mixture was stirred at 60 °C overnight prior to carrying out the film deposition. The thin film of ZnO precursor was annealed at 200 °C for 10 min in air. The active layer was spin-cast from a mixture of IND-DHT-BDT or IND-DHT-BDTF and Y6BO in which the mixture was prepared to stir IND-DHT-BDT (6mg) and Y6BO (8mg) in 1mL of chloroform with 0.5% (v/v) 1-chloronaphthalene (CN) at 2600 rpm for 60s. IND-DHT-BDTF (6 mg) and Y6BO (6 mg) in 1 mL of chloroform with 0.5% (v/v) 1-chloronaphthalene (CN) at 3000 rpm for 60 s. Prior to spin coating, the active solution was filtered through a 0.2 μm membrane filter. This film was preheated at 110 °C for 10min in N₂. Lastly, the MoO₃ (3 nm) and Ag (100 nm) were thermal evaporated at 2 × 10⁻⁶ Torr with a device area was 9 mm².

III.iii Results and discussion

III.iii.1 Optical and Electrochemical properties.

The UV-visible spectra of both donors exhibit broad absorption in the visible region both as a solid thin film (**Figure III -1** (a)) and in the diluted CF solution (**Figure III -1** (b)). The absorption peaks of the IND-DHT-BDT films are 425, and 585 nm and that of the IND-DHT-BDTF films are 431, 582nm, respectively. Both polymer donors can harvest the short wavelength region from 380nm to 650nm. Compared to IND-DHT-BDT, IND-DHT-BDTF is red-shifted in both films and solutions because it has strong intramolecular charge transfer (ICT) stemming from fluorine groups in electron-withdrawing moiety. The optical band gaps of IND-DHT-BDT and IND-DHT-BDTF are 1.86V.

The energy levels of donor polymers are estimated from the onset of cyclic voltammogram (**Figure III -1** (c) and (d)). The highest occupied molecular orbital (HOMO) and lowest unoccupied molecular orbital (LUMO) energy levels of IND-HT-BDT and IND-DHT-BDTF are -5.12/-3.64 eV and -5.14/-3.5 eV, respectively. As shown in energy diagram (**Figure III -1** (e)). The results are summarized in **Table III**.

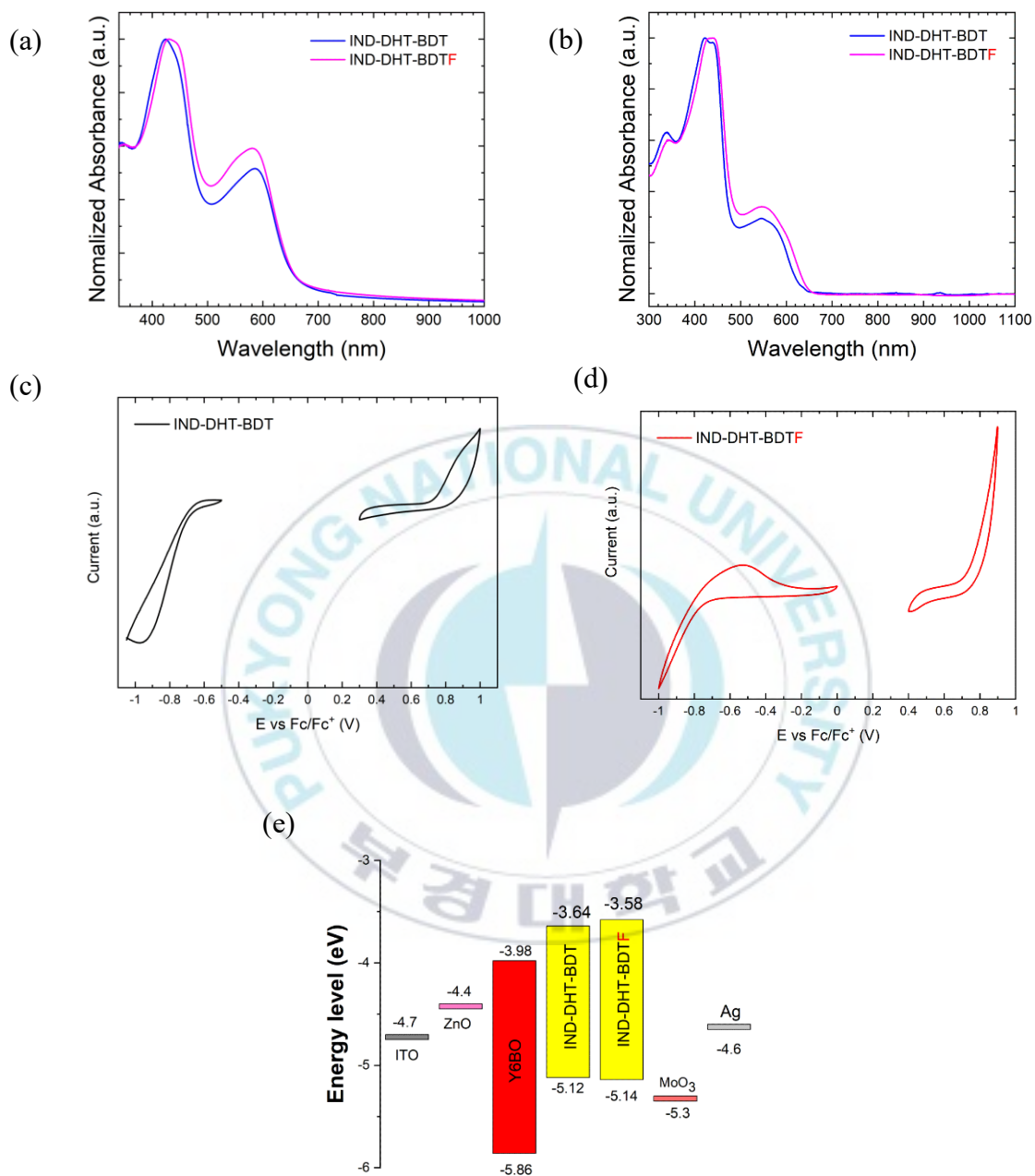


Figure III-I. UV-visible spectra of polymer donors (a) thin films on glass substrates and (b) solution in chloroform and Cyclic voltammograms of (c) IND-DHT-BDT, (d) IND-DHT-BDTF and corresponding (e) energy diagram

Table III Summary of optical and electrochemical properties of the polymer.

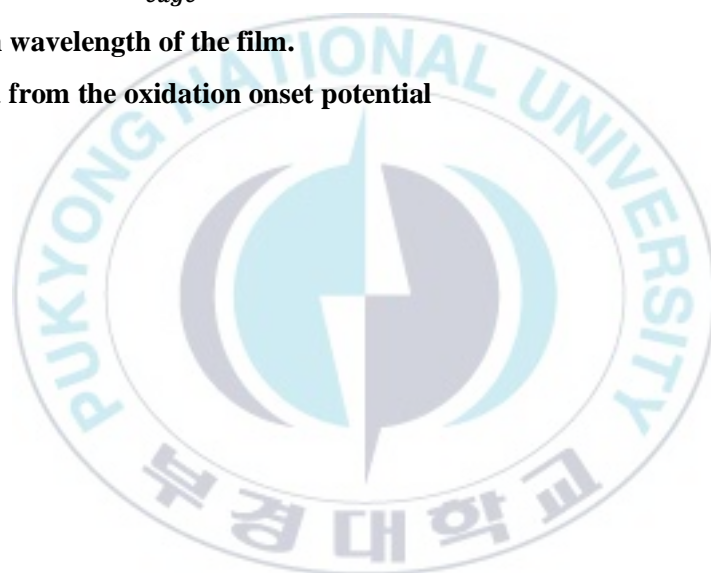
	λ_{edge} (nm) ^a	$\lambda_{max}^{solution}$ (nm)	HOMO (eV) ^c	LUMO (eV) ^d
	E_{gap}^{opt} (eV) ^b	λ_{max}^{film} (nm)		
IND-DHT-IND	666	422, 544	-5.65	-3.56
	1.86	425, 585		
IND-DHT-BDTF	668	440, 547	-5.67	-3.58
	1.86	431, 582		

^a Absorption edge of the film.

^b Estimated from the λ_{edge}

^c Maximum wavelength of the film.

^d Estimated from the oxidation onset potential



III.iii.2 Photovoltaic properties.

The inverted type devices based on ITO/ZnO/donor: Y6BO/MoO₃/Ag was fabricated to investigate the photovoltaic properties of IND-DHT-BDT and IND-DHT-BDTF. The optimized condition of based IND-DHT-BDT devices under AM 1.5G illumination is estimated as 3:4 (w/w) with 0.5% (v/v) 1-chloronaphthelene (CN), that of based IND-DHT-BDTF devices under AM 1.5G illumination is estimated as 3:3 (w/w) with 0.5% (v/v) 1-chloronaphthelene (CN). The J-V plots of both devices are shown in **Figure III-3** (a) and the results are summarized in **Table IV**.

The device based on IND-DHT-BDT: Y6BO device exhibit a J_{sc} of 13.36 mA/cm², a V_{oc} of 0.84 V, a Fill Factor (FF) of 42.65%, and a PCE of 4.79%. In case of IND-DHT-BDTF: Y6BO device, it shows a J_{sc} of 10.22 mA/cm², a V_{oc} of 0.85 V, a FF of 45.6%, and a PCE of 3.96%. The series resistance (R_s) was obtained from the J-V curves obtained under 1.0 sun condition (Shown in **Table IV**)⁴⁵. The series resistance (R_s) followed the tendency of the photovoltaic performances, which are shown in **Table IV**. Incident photon to current efficiency (IPCE) curves (**Figure III-3**) of the devices showed good agreement with the short-circuit current density (J_{sc}) and the performances of the devices (PCE).

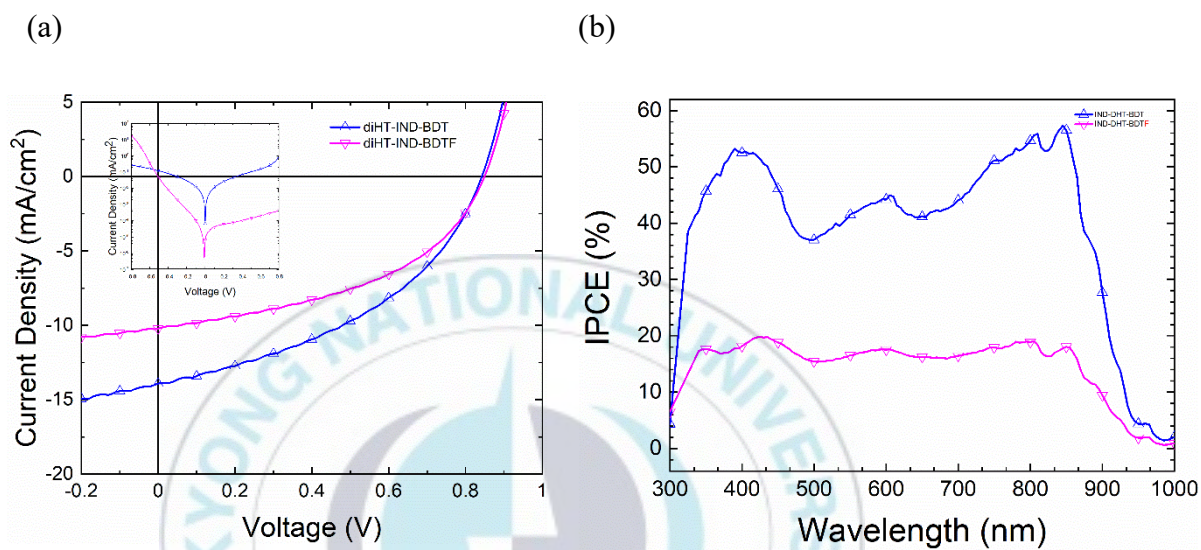
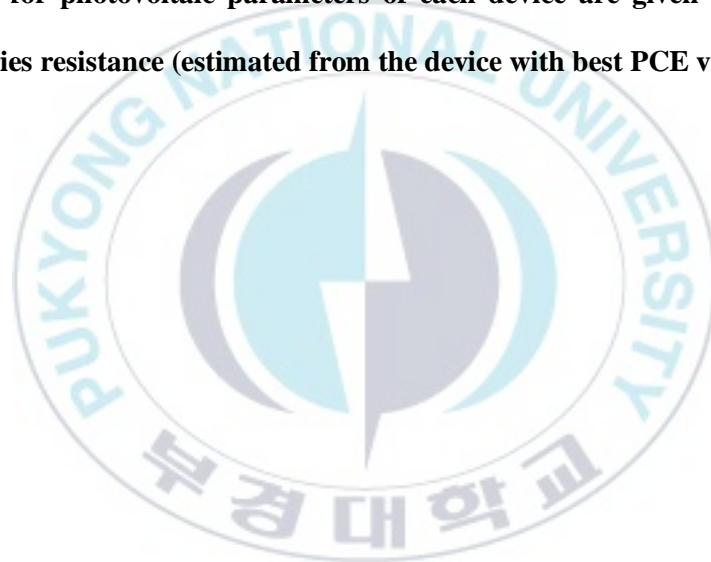


Figure III-XVXVIXVII UV-visible spectra of polymer donors (a) thin films on glass substrates and (b) solution in chloroform and Cyclic voltammograms of (c) IND-DHT-BDT, (d) IND-DHT-BDTF and corresponding (e) energy diagram.

Table IV The best photovoltaic parameters of the PSCs. The averages for the photovoltaic parameters of each device are given in parentheses

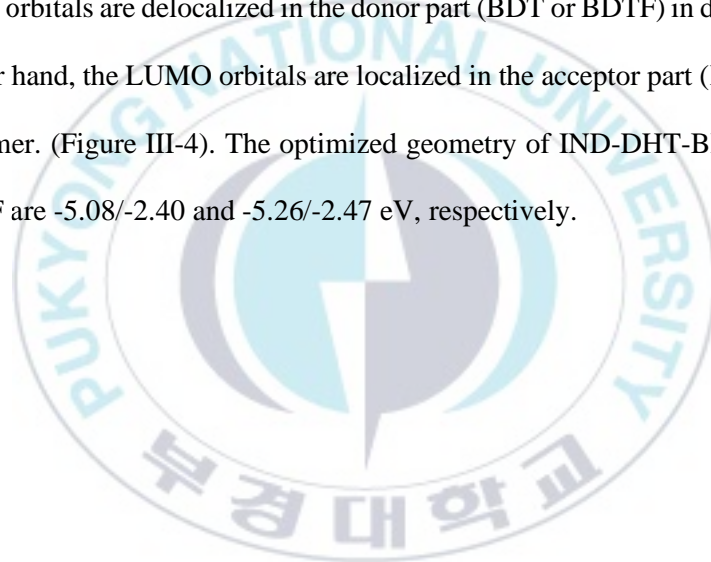
polymer	J_{sc} (mA/cm ²)	V_{oc} (V)	FF (%)	PCE (%)	R_s (Ω cm ²) ^b
IND-DHT-BDT :	13.36	0.84	42.65	4.79	5.96
Y6BO	(13.02)	(0.85)	(42.28)	(4.74)	
IND-DHT-BDT F :	10.22	0.85	45.6	3.96	6.82
Y6BO	(9.76)	(0.85)	(45.77)	(3.81)	

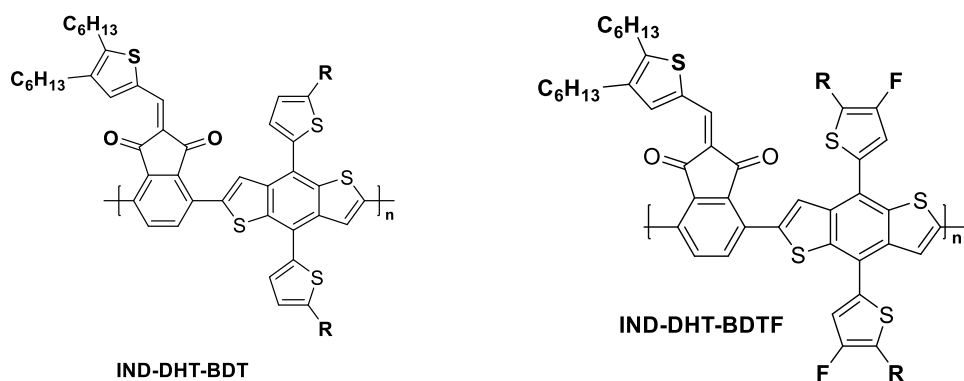
^aThe averages for photovoltaic parameters of each device are given in parentheses with mean variation. ^bSeries resistance (estimated from the device with best PCE value).



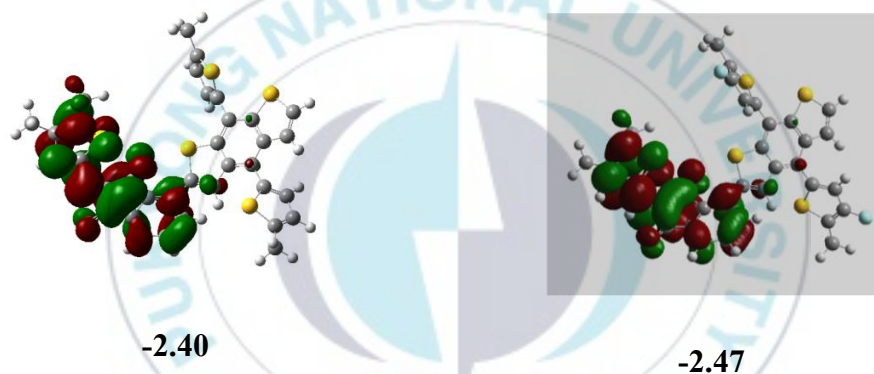
III.iii.3 Computational calculation

Computational calculations based on density functional theory (DFT) were employed to explore the electronic distribution and backbone conformation. The DFT calculations were performed using Gaussian 09 software with the hybrid B3LYP correlation functional and split valence 6-31G(d) basis set.⁴⁶ The electronic distributions and optimized geometries of polymer donors are depicted in Figure II-3. The HOMO orbitals are delocalized in the donor part (BDT or BDTF) in donor polymer. On the other hand, the LUMO orbitals are localized in the acceptor part (IND-DHT) in donor polymer. (Figure III-4). The optimized geometry of IND-DHT-BDT and IND-DHT-BDTF are -5.08/-2.40 and -5.26/-2.47 eV, respectively.





LUMO



HOMO

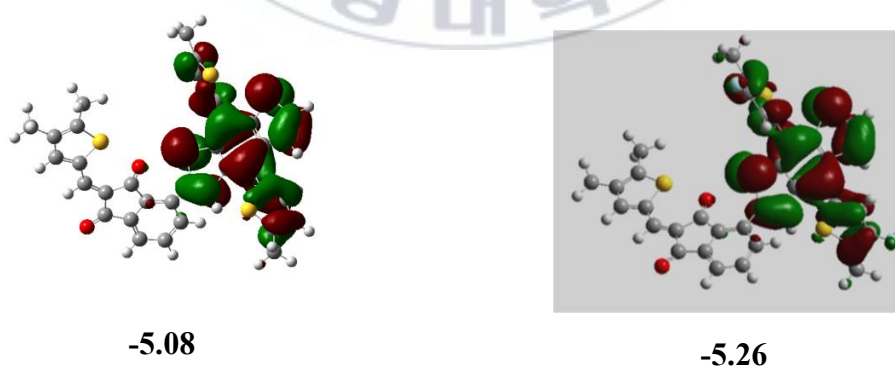


Figure III-XVIII. The electronic distributions of polymer donors obtained from density functional theory (DFT) calculations.

III.iv Conclusion

In this work, we designed and synthesized conjugated donor materials based on Indandione with BDT or BDTF, named IND-DHT-BDT, IND-DHT-BDTF for organic solar cells. Previous study we got good performance, so we decide to introduce one more alkyl part in thiophene, 2,3-dihexylthiophene. The 2,3-dihexyl-thiophene as an electron-donating group, when combined with IND, can effectively form a powerful push-pull structure that induces effective ICT and enhanced optical absorption. The IND-DHT-BDT based devices PCE increased than IND-DHT-BDT, because Introducing the one more alkyl part makes to slightly better solubility, so it makes J_{sc} 12.60 to 13.36 mA/cm². but IND-DHT-BDTF cases decreased J_{sc} and FF. The PCEs of the devices based on polymer donors with BDT were better. Polymer donors with Y6BO enhanced push-pull structure and show a broad light absorption range as well as good solubility. After being added to CN, the PCE of IND-DHT-BDT: Y6BO based device was greatly improved up to 4.79%. These results indicate that side chain engineering is an effective way to further improve the photovoltaic performance of PSCs

Ref.

- [1] Gervet, B. (2007) Coal Fire Emission Contributes to Global Warming, 2007.
- [2] Liang, Y., Xu, Z., Xia, J., Tsai, S.T., Wu, Y., Li, G., et al. (2010) For the bright future-bulk heterojunction polymer solar cells with power conversion efficiency of 7.4%. *Advanced Materials*. 22 (20), 135–138.
- [3] Carlson, D.E. and Wronski, C.R. (1976) Amorphous silicon solar cell. *Applied Physics Letters*. 28 (11), 671–673.
- [4] Yu, B., Shi, J., Tan, S., Cui, Y., Zhao, W., Wu, H., et al. (2021) Efficient (>20 %) and Stable All-Inorganic Cesium Lead Triiodide Solar Cell Enabled by Thiocyanate Molten Salts. *Angewandte Chemie - International Edition*. 60 (24), 13436–13443.
- [5] Ren, Y., Sun, D., Cao, Y., Tsao, H.N., Yuan, Y., Zakeeruddin, S.M., et al. (2018) A Stable Blue Photosensitizer for Color Palette of Dye-Sensitized Solar Cells Reaching 12.6% Efficiency. *Journal of the American Chemical Society*. 140 (7), 2405–2408.
- [6] Zhang, T., An, C., Bi, P., Lv, Q., Qin, J., Hong, L., et al. (2021) A Thiadiazole-Based Conjugated Polymer with Ultradeep HOMO Level and Strong Electroluminescence Enables 18.6% Efficiency in Organic Solar Cell. *Advanced Energy Materials*. 11 (35), 1–8.
- [7] Semonin, O.E., Nozik, A.J., and Beard, M.C. (2013) in a Quantum Dot Solar Cell. *Science*. 1530 (2011), 1530–1534.
- [8] Keshtov, M.L., Kuklin, S.A., Zou, Y., Dahiya, H., Agrawal, A., and Sharma, G.D. (2022) Wide bandgap D-A copolymers with same medium dithieno [2,3-e;3'2'-g]isoindole-7,9 (8H) acceptor and different donors for high-performance fullerene free polymer solar cells with efficiency up to 14.76%. *Chemical Engineering Journal*. 427 (May 2021),.
- [9] Kim, M., Yi, M., Jang, W., Kim, J.K., and Wang, D.H. (2020) Acidity Suppression of Hole Transport Layer via Solution Reaction of Neutral PEDOT:PSS for Stable Perovskite Photovoltaics. *Polymers*. 12 (1), 129.
- [10] Zang, Y., Xin, Q., Zhao, J., and Lin, J. (2018) Effect of Active Layer Thickness on the Performance of Polymer Solar Cells Based on a Highly Efficient Donor Material of PTB7-Th. *Journal of Physical Chemistry C*. 122 (29), 16532–16539.

- [11] Abdulrazzaq, O.A., Saini, V., Bourdo, S., Dervishi, E., and Biris, A.S. (2013) Organic solar cells: A review of materials, limitations, and possibilities for improvement. *Particulate Science and Technology*. 31 (5), 427–442.
- [12] Yu, G. and Wudl, F. (1995) _reports _ _ . (December), 1789–1792.
- [13] Ram, K.S. and Singh, J. (2020) Over 20% Efficient and Stable Non-Fullerene-Based Ternary Bulk-Heterojunction Organic Solar Cell with WS₂ Hole-Transport Layer and Graded Refractive Index Antireflection Coating. *Advanced Theory and Simulations*. 3 (6), 1–8.
- [14] Lungenschmied, C., Dennler, G., Neugebauer, H., Sariciftci, S.N., Glatthaar, M., Meyer, T., et al. (2007) Flexible, long-lived, large-area, organic solar cells. *Solar Energy Materials and Solar Cells*. 91 (5), 379–384.
- [15] Menke, S.M., Ran, N.A., Bazan, G.C., and Friend, R.H. (2018) Understanding Energy Loss in Organic Solar Cells: Toward a New Efficiency Regime. *Joule*. 2 (1), 25–35.
- [16] Qi, B. and Wang, J. (2013) Fill factor in organic solar cells. *Physical Chemistry Chemical Physics*. 15 (23), 8972–8982.
- [17] Han, Y.W., Jeon, S.J., Lee, H.S., Park, H., Kim, K.S., Lee, H.W., et al. (2019) Evaporation-Free Nonfullerene Flexible Organic Solar Cell Modules Manufactured by An All-Solution Process. *Advanced Energy Materials*. 9 (42), 1–15.
- [18] Xue, R., Zhang, J., Li, Y., and Li, Y. (2018) Organic Solar Cell Materials toward Commercialization. *Small*. 14 (41), 1–24.
- [19] Cheng, Y.J., Yang, S.H., and Hsu, C.S. (2009) Synthesis of conjugated polymers for organic solar cell applications. *Chemical Reviews*. 109 (11), 5868–5923.
- [20] Servaites, J.D., Ratner, M.A., and Marks, T.J. (2011) Organic solar cells: A new look at traditional models. *Energy and Environmental Science*. 4 (11), 4410–4422.
- [21] Sun, S., Fan, Z., Wang, Y., and Haliburton, J. (2005) Organic solar cell optimizations. *Journal of Materials Science*. 40 (6), 1429–1443.

- [22] Alam, S., Shaheer Akhtar, M., Abdullah, Eunbi-Kim, Shin, H.S., and Ameen, S. (2020) New energetic indandione based planar donor for stable and efficient organic solar cells. *Solar Energy*. 201 (January), 649–657.
- [23] Abdullah, Ameen, S., Akhtar, M.S., Fijahi, L., Kim, E.B., and Shin, H.S. (2019) Solution processed bulk heterojunction organic solar cells using small organic semiconducting materials based on fluorene core unit. *Optical Materials*. 91 (April), 425–432.
- [24] Chen, X., Feng, H., Lin, Z., Jiang, Z., He, T., Yin, S., et al. (2017) Impact of end-capped groups on the properties of dithienosilole-based small molecules for solution-processed organic solar cells. *Dyes and Pigments*. 147 183–189.
- [25] Holcombe, T.W., Norton, J.E., Rivnay, J., Woo, C.H., Goris, L., Piliago, C., et al. (2011) Steric control of the donor/acceptor interface: Implications in organic photovoltaic charge generation. *Journal of the American Chemical Society*. 133 (31), 12106–12114.
- [26] Zhang, Z., Feng, L., Xu, S., Yuan, J., Zhang, Z.G., Peng, H., et al. (2017) Achieving over 10% efficiency in a new acceptor ITTC and its blends with hexafluoroquinoxaline based polymers. *Journal of Materials Chemistry A*. 5 (22), 11286–11293.
- [27] Wu, Y., Zhang, X., Li, W., Wang, Z.S., Tian, H., and Zhu, W. (2012) Hexylthiophene-featured D-A- π -a structural indoline chromophores for coadsorbent-free and panchromatic dye-sensitized solar cells. *Advanced Energy Materials*. 2 (1), 149–156.
- [28] Cho, S.N., Lee, W.H., Park, J.B., Kim, J.H., Hwang, D.H., and Kang, I.N. (2015) Synthesis and characterization of fluorine atom substituted new BDT-based polymers for use in organic solar cells. *Synthetic Metals*. 210 273–281.
- [29] Bogdanović, G.A., Spasojević-de Biré, A., and Zarić, S.D. (2002) Evidence based on crystal structures and calculations of a C-H $\cdots\pi$: Interaction between an organic moiety and a chelate ring in transition metal complexes. *European Journal of Inorganic Chemistry*. (7), 1599–1602.

- [30] Sarkar, S., Siddiqui, A.A., Saha, S.J., De, R., Mazumder, S., Banerjee, C., et al. (2016) Antimalarial activity of small-molecule benzothiazole hydrazones. *Antimicrobial Agents and Chemotherapy*. 60 (7), 4217–4228.
- [31] Fijahi, L., Shaheer Akhtar, M., Abdullah, Kim, E.B., Seo, H.K., Shin, H.S., et al. (2020) Investigation of newly designed asymmetric chromophore in view of power conversion efficiency improvements for organic solar cells. *Materials Letters*. 260 126865.
- [32] Yao, H., Ye, L., Zhang, H., Li, S., Zhang, S., and Hou, J. (2016) Molecular design of benzodithiophene-based organic photovoltaic materials. *Chemical Reviews*. 116 (12), 7397–7457.
- [33] Xiao, L.N., Wang, L.M., Shan, X.N., Guo, H.Y., Fu, L.W., Hu, Y.Y., et al. (2015) Secondary organic moiety templated organic-inorganic polyoxometalate-based frameworks. *CrystEngComm*. 17 (6), 1336–1347.
- [34] Ye, L., Zhang, S., Huo, L., Zhang, M., and Hou, J. (2014) Molecular design toward highly efficient photovoltaic polymers based on two-dimensional conjugated benzodithiophene. *Accounts of Chemical Research*. 47 (5), 1595–1603.
- [35] Su, N., Ma, R., Li, G., Liu, T., Feng, L.W., Lin, C., et al. (2021) High-Efficiency All-Polymer Solar Cells with Poly-Small-Molecule Acceptors Having π -Extended Units with Broad Near-IR Absorption. *ACS Energy Letters*. 6 (2), 728–738.
- [36] Collins, B.A., Li, Z., Tumbleston, J.R., Gann, E., Mcneill, C.R., and Ade, H. (2013) Absolute measurement of domain composition and nanoscale size distribution explains performance in PTB7:PC71bm solar cells. *Advanced Energy Materials*. 3 (1), 65–74.
- [37] Kim, W., Kim, J.K., Kim, E., Ahn, T.K., Wang, D.H., and Park, J.H. (2015) Conflicted effects of a solvent additive on PTB7:PC71BM bulk heterojunction solar cells. *Journal of Physical Chemistry C*. 119 (11), 5954–5961.
- [38] Ma, W., Yang, G., Jiang, K., Carpenter, J.H., Wu, Y., Meng, X., et al. (2015) Influence of Processing Parameters and Molecular Weight on the Morphology and Properties of High-Performance PffBT4T-2OD:PC71BM Organic Solar Cells. *Advanced Energy Materials*. 5 (23), 1–9.

- [39] Liu, F., Li, C., Li, J., Wang, C., Xiao, C., Wu, Y., et al. (2020) Ternary organic solar cells based on polymer donor, polymer acceptor and PCBM components. *Chinese Chemical Letters*. 31 (3), 865–868.
- [40] Zhang, G., Chen, X.K., Xiao, J., Chow, P.C.Y., Ren, M., Kupgan, G., et al. (2020) Delocalization of exciton and electron wavefunction in non-fullerene acceptor molecules enables efficient organic solar cells. *Nature Communications*. 11 (1), 1–10.
- [41] Lin, Y., Wang, J., Zhang, Z.G., Bai, H., Li, Y., Zhu, D., et al. (2015) An electron acceptor challenging fullerenes for efficient polymer solar cells. *Advanced Materials*. 27 (7), 1170–1174.
- [42] Bao, Z., Chan, W.K., and Yu, L. (1995) Exploration of the Stille Coupling Reaction for the Syntheses of Functional Polymers. *Journal of the American Chemical Society*. 117 (50), 12426–12435.
- [43] Hasnidawani, J.N., Azlina, H.N., Norita, H., Bonnia, N.N., Ratim, S., and Ali, E.S. (2016) Synthesis of ZnO Nanostructures Using Sol-Gel Method. *Procedia Chemistry*. 19 211–216.
- [44] He, Q., Shahid, M., Jiao, X., Gann, E., Eisner, F.D., Wu, T., et al. (2020) Crucial Role of Fluorine in Fully Alkylated Ladder-Type Carbazole-Based Nonfullerene Organic Solar Cells. *ACS Applied Materials and Interfaces*. 12 (8), 9555–9562.
- [45] Pysch, D., Mette, A., and Glunz, S.W. (2007) A review and comparison of different methods to determine the series resistance of solar cells. *Solar Energy Materials and Solar Cells*. 91 (18), 1698–1706.
- [46] Sieffert, N., Wipff, G., Revision, D., Frisch, M.J., Trucks, G.W., Schlegel, H.B., et al. (2014) Uranyl Extraction by N, N -Dialkylamide Ligands Studied by Static and Dynamic DFT Simulations - Supporting Information -. (November), 1–15.
- [47] Ye, D., Rongpipi, S., Kiemle, S.N., Barnes, W.J., Chaves, A.M., Zhu, C., et al. (2020) Preferred crystallographic orientation of cellulose in plant primary cell walls. *Nature Communications*. 11 (1), 1–10.
- [48] Lenes, M., Morana, M., Brabec, C.J., and Blom, P.W.M. (2009) Recombination-limited photocurrents in low bandgap polymer/fullerene solar cells. *Advanced Functional Materials*. 19 (7), 1106–1111.

- [49] Rao, A., Chow, P.C.Y., Gélinas, S., Schlenker, C.W., Li, C.Z., Yip, H.L., et al. (2013) The role of spin in the kinetic control of recombination in organic photovoltaics. *Nature*. 500 (7463), 435–439.
- [50] Sagita, C.P., Lee, J.H., Lee, S.W., Whang, D.R., Kim, J.H., and Chang, D.W. (2021) Enhanced photovoltaic performance of quinoxaline-based donor-acceptor type polymers with monocyano substituent. *Journal of Power Sources*. 491 (February), 229588.
- [51] Wardani, R.P., Jeong, M., Lee, S.W., Whang, D.R., Kim, J.H., and Chang, D.W. (2021) Simple methoxy-substituted quinoxaline-based D-A type polymers for nonfullerene polymer solar cells. *Dyes and Pigments*. 192 (January), 109346.
- [52] Sun, C., Pan, F., Bin, H., Zhang, J., Xue, L., Qiu, B., et al. (2018) A low cost and high performance polymer donor material for polymer solar cells. *Nature Communications*. 9 (1), 1–10.
- [53] Wang, G., Eastham, N.D., Aldrich, T.J., Ma, B., Manley, E.F., Chen, Z., et al. (2018) Photoactive Blend Morphology Engineering through Systematically Tuning Aggregation in All-Polymer Solar Cells. *Advanced Energy Materials*. 8 (12), 1–13.
- [54] Wang, Y., Yan, Z., Guo, H., Uddin, M.A., Ling, S., Zhou, X., et al. (2017) Effects of Bithiophene Imide Fusion on the Device Performance of Organic Thin-Film Transistors and All-Polymer Solar Cells. *Angewandte Chemie - International Edition*. 56 (48), 15304–15308.
- [55] Hwang, Y.J., Earmme, T., Courtright, B.A.E., Eberle, F.N., and Jenekhe, S.A. (2015) n-Type Semiconducting Naphthalene Diimide-Perylene Diimide Copolymers: Controlling Crystallinity, Blend Morphology, and Compatibility Toward High-Performance All-Polymer Solar Cells. *Journal of the American Chemical Society*. 137 (13), 4424–4434.
- [56] Jung, J.W., Jo, J.W., Chueh, C.C., Liu, F., Jo, W.H., Russell, T.P., et al. (2015) Fluoro-substituted n-type conjugated polymers for additive-free all-polymer bulk heterojunction solar cells with high power conversion efficiency of 6.71%. *Advanced Materials*. 27 (21), 3310–3317.

- [57] Zhao, W., Li, S., Yao, H., Zhang, S., Zhang, Y., Yang, B., et al. (2017) Molecular Optimization Enables over 13% Efficiency in Organic Solar Cells. *Journal of the American Chemical Society*. 139 (21), 7148–7151.



Acknowledgment

짧다면 짧고 길다면 긴 2 년간의 석사생활에 성취를 이루고 대학원에 진학하여 만난 수많은 인연들이 너무나도 소중하고 감사의 말씀을 전해드리고 싶습니다

여러모로 많이 부족하고 실수도 잦은 저를 여기까지 이끌어 주신 **김주현 교수님**께 깊이 감사의 말씀을 드립니다. 또한 좋은 가르침들을 주신 많은 고분자공학과 교수님들께도 감사드립니다.

처음 연구실을 들어오기를 권해주었던 **호철이**, 모르는 부분과 많은 것을 알려주었던 **미진이**, 많은 질문을 하여도 웃으며 대답해주었던 **준호**, 부족한 영어와 사수로써 많이 도와준 **라트나**와 처음부터 끝까지 같이 있어준 **사브리나**, 영어를 많이 알려준 **라마**, 항상 어른스러운 **아날리아**, 항상 에너지 넘치고 맨날 싸우는 **아유니**, 열심히 하는 **승건이**까지 연구실 생활에 많은 소중한 사람들 감사합니다.

그리고 항상 저를 믿어 주시고 지지해주시는 **부모님과 형, 동생**, 항상 에너지가 넘치고 감당해야하는 **연화**, 가장 어른스럽고 바쁜 **지원이**, 우리 찌모델 **호철이**, 학부생부터 지금까지 항상 옆에 있어주던 **동현이, 민섭이형, 선우형, 동엽이형, 준성이형, 민웅이**, 타지였던 부산생활에서 힘이 많이 되었던 **모세**, 고향 가면 항상 반겨주던 **대현이, 종현이, 준민이, 영수, 지은이, 아영이** 등 너무 감사한 분들이 많아 미처 언급하지 못한 많은 분들께도 무한한 감사의 말씀을 전합니다.

덕분에 힘든 일도 견딜 수 있었고 너무 행복하였습니다. 감사합니다.

2022 년 2 월

손동환 올림